Title

An updated end-to-end ecosystem model of the Northern California Current reflecting ecosystem changes due to recent marine heat waves

Authors

Dylan G.E. Gomes[1,2], James J. Ruzicka[3], Lisa G. Crozier[4], David D. Huff[5], Elizabeth M. Phillips[6], Pierre-Yves Hernvann[7,8], Cheryl A. Morgan[2], Richard D. Brodeur[5], Jen E. Zamon[9], Elizabeth A. Daly[2], Joseph. J. Bizzarro[10, 11], Jennifer L. Fisher[5], Toby D. Auth[12]

[1] National Academy of Sciences NRC Research Associateship Program, Northwest Fisheries Science Center, National Marine Fisheries Service, National Oceanic and Atmospheric Administration, Seattle, WA, USA 98112

[2] Cooperative Institute for Marine Ecosystem and Resources Studies, Hatfield Marine Science Center, Oregon State University, Newport, OR, USA 97365

[3] Ecosystem Sciences Division, Pacific Islands Fisheries Science Center, National Marine Fisheries Service, National Oceanic and Atmospheric Administration, Honolulu, HI, USA 96822

[4] Fish Ecology Division, Northwest Fisheries Science Center, National Marine Fisheries Service, National Oceanic and Atmospheric Administration, Seattle, WA, USA 98112

[5] Fish Ecology Division, Northwest Fisheries Science Center, National Marine Fisheries Service, National Oceanic and Atmospheric Administration, Newport, OR, USA 97365

[6] Fishery Resource Analysis and Monitoring Division, Northwest Fisheries Science Center, National Marine Fisheries Service, National Oceanic and Atmospheric Administration, Seattle, WA, USA 98112

[7] Conservation Biology Division, Northwest Fisheries Science Center, National Marine Fisheries Service, National Oceanic and Atmospheric Administration, Newport, OR, USA 97365

[8] Institute of Marine Sciences, University of California, Santa Cruz, Santa Cruz, CA, USA

[9] Fish Ecology Division, Point Adams Research Station, Northwest Fisheries Science Center, National Marine Fisheries Service, National Oceanic and Atmospheric Administration, Hammond, OR, USA 97121

[10] Fisheries Ecology Division, Southwest Fisheries Science Center, National Marine Fisheries Service, National Oceanic and Atmospheric Administration, Santa Cruz, CA, USA 95064

[11] Fisheries Collaborative Program, University of Santa Cruz, Santa Cruz, CA, USA 95060

[12] Pacific States Marine Fisheries Commission, Newport, OR, USA 97365

[*] Corresponding author: dylan.gomes@noaa.gov

Abstract

The Northern California Current is a highly productive marine upwelling ecosystem that is economically and ecologically important. It is home to both commercially harvested species and those that are federally listed under the U.S. Endangered Species Act. Recently, there has been a global shift from single-species fisheries management to ecosystem-based fisheries management, which acknowledges that more complex dynamics can reverberate through a food web. Here, we have integrated new research into an end-to-end ecosystem model (i.e., physics to fisheries) using data from long-term ocean surveys, phytoplankton satellite imagery paired with a vertically generalized production model, a recently assembled diet database, fishery catch information, species distribution models, and existing literature. This spatially-explicit model includes 90 living and detrital functional groups ranging from phytoplankton, krill, and forage fish to salmon, seabirds, and marine mammals, and nine fisheries that occur off the coast of Washington, Oregon, and Northern California. This model was updated from previous regional models to account for more recent changes in the Northern California Current (e.g., increases in market squid and some gelatinous zooplankton such as pyrosomes and salps), to expand the previous domain to increase the spatial resolution, to include data from previously unincorporated surveys, and to add improved characterization of endangered species, such as Chinook salmon (*Oncorhynchus tshawytscha*) and southern resident killer whales (*Orcinus*

orca). Our model is mass-balanced, ecologically plausible, without extinctions, and stable over 100-year simulations. Ammonium and nitrate availability, total primary production rates, and model-derived phytoplankton time series are within realistic ranges. As we move towards holistic ecosystem-based fisheries management, we must continue to openly and collaboratively integrate our disparate datasets and collective knowledge to solve the intricate problems we face. As a tool for future research, we provide the data and code to use our ecosystem model.

Keywords

marine food web; marine food-web; biological oceanography; multi-species interaction; NCC; ECOTRAN; Ecopath; Ecosim; Ecospace; EwE; Atlantis; global change; climate change

Table of contents

Title 1
Authors 1
Abstract 2
Keywords 3
Introduction 6
Methods 8
- Model Background 8
- Physical Model Structure and Model Drivers 9
- Mass-balancing 11
- Biomass density 15
- Functional group data processing 16
  - Phytoplankton 16
  - Zooplankton, jellies, and pyrosomes 17
  - Krill and shrimp 19
  - Juvenile fish 19
  - Coastal pelagic fish 20
  - Salmonids 20
  - Hake 21
  - Groundfish and crabs 21
  - Seabirds 21
  - Marine mammals 22
  - Model-estimated groups 22
- Diet matrix 23
  - Marine mammal diets 26
- Fisheries landings 26
- Tuning detritus recycling 28
- Model validation 29

Results 31
Discussion 33
Data availability statement 39
Acknowledgements 39
Funding 40
References 41

Supporting Information 55
Appendix 55
Biomass sources 55
Coastal Pelagic Species 55
Pacific Hake Ecosystem Acoustic Trawl Survey 56
Juvenile Salmon and Ocean Ecosystem Survey (JSOES) 56
Newport Hydrographic Line 57
Pre-recruit survey 58
West Coast Groundfish Bottom Trawl Survey 59
Diet sources 59
California Current Trophic Database 59
Juvenile salmon diets 60
Tables 62
Table 1: NCC EcoTran parameters. 62
Table 2: Functional group definitions. 68
Figures 74
Fig 1: Map of Northern California Current 74
Fig 2: Cross-shelf physical model 75
Fig 3: Subregional heatmaps of functional group spatial distributions 76
Fig 4: Biomass density and trophic level of model functional groups 79
Fig 5: Diet matrix of ecosystem model by trophic level 81
Fig 6: EcoTran trophic network of ecosystem model 83
Fig 7: EcoTran trophic network of non-detritus groups by trophic level 84
Fig 8: Validation; Biomass-specific production and consumption values by trophic level 86
Fig 9: 100-year model simulation driven by average upwelling time series 89
Fig 10: Primary production time series as both ecosystem model output and vertically generalized production model 91

Introduction

The Northern California Current (NCC) marine ecosystem extends from Vancouver Island, British Columbia to Cape Mendocino, California and is a highly productive upwelling ecosystem that is economically and ecologically important [1,2]. This ecosystem has recently experienced multiple biophysical stressors: an increase in water temperatures [3], seasonally low oxygen [4,5], decreased pH and calcium carbonate saturation state (i.e., ocean acidification) [6,7], increased magnitude and frequency of marine heatwaves (i.e., the 2014-2016 and 2019-2020 marine heatwaves) [8–10], and coastwide harmful algal blooms [11,12] that cumulatively have resulted in dramatic changes to the ecosystem [13–16]. Climate change is expected to continue to exacerbate these issues within the NCC in complex ways [17,18], which is a cause for concern as the NCC is home to many commercially and recreationally important species as well as taxa listed under the Endangered Species Act (ESA) [19–21].

Over the last 30 years, there has been a growing recognition of the importance of holistic, ecosystem-based management [22–24]. Additionally, improved availability of long-term datasets, increased computing power, and advances in quantitative tools have allowed a heightened focus on multi-species and ecosystem-based management approaches that consider complex trophic interactions, incorporate physical oceanographic processes, and integrate multiple disparate data sources and their uncertainties [23,25–30]. Ecosystem models have been used to address fisheries management questions because they track energy flow through modeled ecosystems, thereby evaluating sensitivities to perturbations of predator-prey interactions and furthering our understanding of poorly studied species, and allowing for the evaluation of long-term management scenarios [31]. In end-to-end ecosystem models, full ecosystems are parameterized

from the physical oceanographic drivers to the trophic interactions within food webs (including fisheries). Advances in end-to-end ecosystem modeling efforts have leveraged multiple ongoing data collection efforts in the NCC to understand how complicated interactions shape ecosystem response to environmental perturbations [7,32–36].

Ecosystems and predator-prey interactions are ever-changing in time and space in concert with fluctuations in climate [37,38]. Thus, for a successful understanding of changing ecosystem states, we must continually update, adapt, or further develop ecosystem models with the most recently available data. Here we update and expand upon previous ecosystem models of the NCC described by Ruzicka et al. (2012, 2016) [32,33] and present an end-to-end ecosystem model using the EcoTran platform [27], which builds upon the widely-used Ecopath framework [25]. We used long-term NCC ship-based surveys and marine mammal stock assessments to derive biomass inputs for 77 of 90 functional groups (from phytoplankton, zooplankton, and micronekton to coastal pelagic fish species and salmon to seabirds, pinnipeds, and killer whales). We focused on data collected primarily during and after recent marine heatwaves (2014 – 2021) to more accurately reflect the current conditions within the NCC, as there is evidence that the ecosystem has entered a novel state [15,16]. We updated the representation of food web interactions with published and unpublished datasets and reports to reflect potential reshuffling of trophic links. We incorporated updated landings data from nine fisheries. We provide detailed descriptions, tables, model code, and visualizations of the ecosystem model. We also demonstrate our ability to represent ecosystem states using model validation metrics and visualizations [30,39]. This new model has potential to become a tool for scientists and managers

interested in the California Current marine ecosystem and will continue to evolve as data sources and information are gathered.

Methods

Model Background

For the purposes of this model, we define the Northern California Current (NCC) domain (Fig 1) to extend latitudinally from Cape Flattery, Washington (48.34N) to just north of Cape Mendocino, in Eureka, California (40.80N) and longitudinally across the shelf from the 1 m to 1280 m isobaths. We define 15 subregions of the model both latitudinally and bathymetrically. That is, the model domain is divided into three bathymetric bins: inner shelf (1 – 100 m depths), mid shelf (101 – 200 m), and outer shelf (201 – 1280 m), and five latitudinal bins: northern California (40.8 – 42 °N), southern Oregon (42 – 44.4 °N), northern Oregon (44.4 – 46 °N), the Columbia River zone (46 – 46.7 °N), and the Washington coast (46.7 – 48.34 °N). The ecosystem model is parameterized with inputs from satellite data, pelagic survey data, fishery data, local diet studies, marine mammal stock assessments, acoustic-trawl and bottom-trawl survey reports from the National Oceanic and Atmospheric Administration's (NOAA) National Marine Fisheries Service (NMFS) –from both the Northwest Fisheries Science Center (NWFSC) and the Southwest Fisheries Science Center (SWFSC), Oregon State University, and various other sources (see below and Table S1). Where possible, we preferentially selected recent years (2014 – present) to parameterize initial conditions. In some cases that was not possible as new data is not readily available, so we relied on a previous version of the NCC food web (see below and Table S1).

We chose to model the functioning of the NCC ecosystem using the EcoTran framework (from Ecopath-Transpose; [27,32,40]. EcoTran is a mass-balanced food-web model that represents the energy flow across ecosystem components and expands upon the well-known Ecopath model [25]. Ecopath solves for the rates of live-weight biomass transfer along each trophic linkage by calculating the consumption demand of consumer groups (grazer or predator) upon each prey group given group biomasses, weight-specific consumption and production rates, and diet compositions. The Ecopath solution for the food web is a matrix describing each consumer group's consumption rate of each producer group. The Ecopath consumption matrix was re-expressed as a trophic network, mapping the fate of all consumed biomass by each functional group among all living consumers, detritus pools, and nitrogenous waste pools via EcoTran techniques (A.K.A. Ecopath-Transpose) [27,32,40]:

$$A_{ji} = \frac{D_{ij}c_j}{\sum_j (D_{ij}c_j)}$$

Equation 1

where A_{ji} = the trophic network matrix (the fraction of total production of each producer i consumed by each consumer j), D_{ij} = the diet matrix (the fraction of each producer i in the diet of each consumer j), and c_j = consumption rate of consumer j. The trophic network matrix A_{ji} was expanded to include detritus and nitrogenous waste (nitrate and ammonium) pools as distinct functional groups.

Physical Model Structure and Model Drivers

EcoTran is a spatially-explicit end-to-end model and allows direct linking of physical oceanographic forcings to the food web model, which drives primary production and the

transport of plankton, detritus, and nutrients across model domain boundaries. We use the 2-dimensional model structure of Ruzicka et al. (2016, 2018) [33,40]. The cross-shelf physical model domain is divided into five sub-regions (Fig 2): box I inner shelf zone of coastal upwelling, boxes II and III mid shelf zone, boxes IV and V outer shelf zone. The mid and outer shelf zones are divided into surface (boxes II and IV) and subsurface layers (boxes III and V) defined by an annual mean mixed layer depth of 15 m [33,40]. Boxes I, II, and IV each contain individual, vertically-integrated food webs representing the complete set of trophic interactions among pelagic and benthic functional groups. Sub-surface boxes III and V are used to account for the physical transport of nutrients, plankton, and detritus particles across the shelf at depth and the loss of sinking detritus from surface boxes (Table S2, S3). Trophic interactions in boxes III and V are limited to the transfer of phytoplankton to detritus via senescence, the metabolism of detritus by bacteria, and the nitrification of ammonium. See Ruzicka et al. (2016, 2018) [33,40] for details.

The currency of a time-dynamic EcoTran model is nitrogen input to the system as nitrate and ammonium at the base of the food web via upwelling and detritus remineralization by bacteria [33]. Nutrients are input to the system via advection flux across the ocean-shelf model domain boundary (boxes IV and V, Fig 2) that are defined by the daily coastal upwelling transport index (CUTI) [41], and by the monthly climatological nitrate and ammonium concentrations observed by the Newport Hydrological Line survey across the central Oregon shelf over years 1998-2008 (46.7° N) [33,42]. Nutrient input drives primary production which, in turn, supports grazing and predation by higher trophic level groups and catch by fishing fleets. Boundary conditions for non-nutrient functional groups are assumed to be identical on both sides of the surface and deep

oceanic boundaries (reflective boundary conditions). There is no net input of non-nutrient biomass into the model domain nor dilution via physical flux of oceanic waters, though non-nutrient biomass can be exported from the model domain to the ocean.

Mass-balancing

After parameterizing functional group biomasses (see below), we compared the model-wide (aggregated across all subregions, hereafter 'aggregated') average biomass values with those from Ruzicka et al. (2012, 2016) [32,33]. When values differed by an order of magnitude, we revisited those datasets and data providers in search of errors in the data cleaning process or in the metadata (e.g., units of measurement). Once obvious errors were fixed or removed, then we attempted to mass-balance the aggregated model. During mass-balancing, imbalance may occur and highlight an insufficient biomass or excedentary production of a given functional group to sustain predation and/or fishing mortality, resulting in a loss or gain of energy in the system. Such imbalance could result from incorrect assumptions, or inaccurate values of the main trophic flow parameters or biomass inputs. The relative reliability of multiple datasets may be assessed by examining whether or not estimates from each source are unbalanced (i.e., a prey group's energy or biomass store is consumed more than the group produces itself).

The physiological rate parameters used by Ecopath to mass-balance the aggregated model are P/B = Biomass-specific Production rate, C/B = Biomass-specific Consumption rate, P/Q = Production efficiency, which can be defined as (P/B) / (C/B), AE = Assimilation Efficiency, and EE = Ecotrophic Efficiency (defined or estimated; Equation 2; Table 1). Most physiological rate

parameters (P/B, C/B, P/Q, and AE) were taken from a previous NCC ecosystem model [32] or borrowed from other trophic models of the northeast-Pacific [31,43,44].

During mass-balancing, the ecotrophic efficiency (EE) is estimated by the Ecopath master equation (Equation 2 below) for most groups [excepting groups where biomass was estimated and EE was fixed (see 'Biomass density' section below) based on common Ecopath assumptions [25,31]] as,

$$B_i\left(\frac{P}{B}\right)_i \times EE_i + I_i + BA_i = \Sigma\left[B_j \times \left(\frac{C}{B}\right)_j \times D_{ij}\right] + E_i + F_i$$

Equation 2

where B_i is the biomass density of prey group i, $(P/B)_i$ is the biomass-specific production rate, EE_i is the Ecotrophic Efficiency for group i, I_i is the immigration rate into the model domain, BA_i is a user-defined biomass accumulation term if biomass is known to be increasing or decreasing over time (for simplicity, we account for no known accumulation over time). Everything on the left side of the equation (i.e., the total production of group i in the system) must be balanced by the loss terms on the right, where B_j is the biomass density of predator group j, $(C/B)_j$ is the biomass-specific consumption rate of predator group j, D_{ij} represents the fraction of prey i consumed by predator j as defined by the diet matrix, E_i is the emigration rate for prey group i, and F_i is the fisheries catch of group i. Σ indicates that everything in the brackets is summed across each predator j for the consumed group i. All of these terms are input parameters of the model, except either B_i or EE_i for each group. That is, only one of these terms is provided and the other is estimated during the mass-balancing process [25,31].

The Ecopath ecotrophic efficiency (EE) is the fraction of a given functional group's production that is used in the system (i.e., not transferred to the detritus), hence between 0 and 1; that is, production is (i) consumed by another functional group or fishing, (ii) moved across model domain boundaries, or (iii) integrated into the functional group's growth as additional biomass. According to the first law of thermodynamics, EE should be between 0 and 1 so that mass-balance is reached. When EE values greater than one were encountered, we balanced the model by either applying scaling factors to survey biomass or by adjusting the diet matrix. Survey biomasses are notoriously underestimated since many animals can avoid sampling gear, and sampling is unlikely to occur at peak activity in the water column for all species surveyed. Thus, relatively large scaling factors are used for small animals (e.g., invertebrate eggs) that can pass through the net more easily or large animals (e.g., adult salmon) that can avoid nets more easily (i.e., estimates are low) and scaling factors near, or precisely, a value of one were used for acoustic-trawl surveys that use targeted trawls to validate acoustic biomass estimates (i.e., estimated biomass is likely more accurate and precise; see "BiomassScalers.csv" in supplement for scaling factors).

Survey biomasses and the diet matrix are imperfect because they are only a snapshot in time and space. Mass-balancing is inherently subjective as we adjust input parameters based on our understanding of survey/study limitations and the data quality (in time, space, methodology, and sampling effort). We were willing to adjust diets that were parameterized with older data (or with fewer samples) more so than diets with newer and more spatially relevant data (or with higher sample sizes). Most diet adjustments during mass-balancing were caused by a precipitous decline

304 in sardine between this model and the previous version (sardine biomass is lower by a factor of
305 more than 8), which wasn't reflected in the outdated diet studies (see
306 "MassBalancingDetails.csv" in supplementary data and code for more details).
307
308 Since gelatinous zooplankton have a greater water content relative to other functional groups
309 [45], their importance to the trophic network may be overestimated in our model (which is
310 expressed in wet-weight biomass during Ecopath model balancing). Thus, the biomass of
311 gelatinous functional groups and diet contributions of these groups as prey to the next trophic
312 level were scaled such that each unit of small gelatinous zooplankton biomass and large
313 carnivorous jellyfish biomass equaled the water content of crustacean zooplankton and pelagic
314 fishes, respectively [34]. Pyrosome data were collected during three different times of year [45].
315 Thus, we used assumptions of seasonal changes in abundance and linear interpolation to generate
316 a yearly average pyrosome density, in combination with the above gelatinous conversion factors,
317 to scale down our overall biomass densities for pyrosomes which were originally calculated from
318 the Pre-recruit survey (see "BiomassScalers.csv", "PyrosomeScaling.csv", "FlowChart.pdf", and
319 "MassBalancingDetails.csv" for more details).
320

321 ## Biomass density

322 Model parameterization and community composition of the model includes 90 functional groups
323 (2 primary producers, 83 consumers, 5 detritus) and 9 fisheries (Table 2). Biomass densities
324 (Table 1) were estimated from survey data for 65 of these groups, values for another 12 groups
325 were borrowed from a previous Northern California Current ecosystem model [32,33], and
326 biomasses of the remaining 13 (of the 90 living and detritus groups) were estimated by the model

327 itself (see Equation 2). Below we describe the data sources for the ecosystem model [46] and our
328 procedure for estimating biomass density from the data provided. Table S1 includes a
329 comprehensive list of biomass density data sources for each functional group.
330
331 All survey data were quality controlled with input from the collectors and maintainers of the
332 datasets. Failing to include absence data would severely overestimate biomass. If absence data
333 were missing (i.e., if data provided only included positive occurrences), we added zero values for
334 all sampled stations that did not include a positive value for any species that was recorded by the
335 survey at another time and location.
336
337 Each survey dataset was used to calculate biomass densities as weight in metric tons per volume
338 of water sampled in cubic kilometers (mt/km^3; details for individual datasets are described
339 below). Volumetric densities were converted to areal densities (mt/km^2; i.e., vertically-integrated
340 densities) by multiplying each volumetric density by assumed vertical distributions for each
341 functional group (see Ruzicka et al., 2012, 2016 [32,33]; depth range assumptions in
342 supplemental data) within each 15 model subregions (Fig 3). We average across individual
343 sampling events within each of the 15 model subregions to obtain values for mass-balancing and
344 as starting points for time dynamic scenarios (Table 1; Fig 4). Because the spatial distribution of
345 many marine organisms is patchy (with infrequent catches of very high abundance or biomass),
346 data can be highly skewed and of high variance. Thus, estimating mean biomass values can be
347 more accurate when based on a log-normal distribution [47]. The delta distribution is a
348 probability distribution used to estimate the mean and variance for a dataset that has both zero
349 and non-zero values; in this case, only the non-zero values follow a log-normal distribution [47].

To derive fish biomass from bottom trawl surveys, we used the delta distribution to account for infrequent catches of large biomass values (highly skewed and of high variance). In contrast, we used the arithmetic mean to derive fish biomass from acoustic-trawl data (i.e., hake and coastal pelagic species, see below) and mid-water tows for zooplankton and other small organisms, as their distribution in the water column is thought to be more uniform, (see "RegionalBiomassCalculator.m" in supplemental code).

Functional group data processing

Phytoplankton

Net primary productivity rates were estimated from satellite images and a vertically generalized production model (VGPM) product (SeaWIFS Chl data; [48,49]). Monthly VGPM products for 2014 – 2021 were downloaded on March 8, 2022 (http://sites.science.oregonstate.edu/ocean.productivity/index.php). Phytoplankton production rate data were trimmed to our model domain using a shapefile of the domain extent (see supplement) and the R package `sp` [50]. Units provided for phytoplankton production rates were mg C / m^2 day^{-1} and were converted to mt / km^2 $year^{-1}$ with phytoplankton-specific carbon–weight conversion factors [51] and standard unit conversions for weight, area, and time (see "BiomassWork/" in the supplemental data and code). Production was then converted to biomass density (mt / km^2) by dividing by the biomass-specific production rates of phytoplankton used in the model (yearly P/B rates in Table 1). We used average phytoplankton biomass density from April – September to parameterize model initial conditions to match the high productivity months during which most biological surveys occurred (see Appendix). The phytoplankton size composition – large (diatom; >10 μm) and small (flagellate; ≤ 10 μm) – were estimated from the

total phytoplankton concentration using a relation between the fraction of small phytoplankton and total Chlorophyll a from observations of the Newport Hydrographic Line (see Appendix for a description of the survey; fraction $P_{small} = 0.30821 \times [\text{Chl a (mg m}^{-3})]^{-0.82351}$; as described in [32].

Zooplankton, jellies, and pyrosomes

Zooplankton were parameterized with the Juvenile Salmon and Ocean Ecosystem Survey (JSOES), Newport Hydrographic Line, and Pre-recruit surveys (see Appendix for survey descriptions). When individual species data came from multiple surveys (see below), calculated biomass densities (for each subregion; Fig 3) were first averaged across surveys (where sampling was spatially overlapping) and then summed within functional groups as average biomass densities for the entire functional group (Table 1, 2).

Crustacean larvae, euphausiid larvae, pelagic (hyperiid and gammarid) amphipods, chaetognaths, ichthyoplankton, and fish eggs were sampled with JSOES bongo nets; copepods, pteropods, ostracods, cladocerans, polychaetes, urochordates, ctenophores and small medusae, mollusk larvae, echinoderm larvae, other small invertebrate larvae and eggs, and other macro-zooplankton were sampled with JSOES vertical nets; and large jellies came from the JSOES fish trawl nets (all data from 2014 – 2021).

Additional data on small invertebrate larvae and invertebrate eggs from the Newport Hydrographic Line (2014 – 2020; May – July) were used to calculate average biomass density values (along with the JSOES data) for all transects that fell within overlapping subregions (Fig

1, 3). Biomass density values for both surveys were provided in units of mg C / m^3 and converted into metric tons / km^3 using group-specific carbon-to-dry-weight and dry-weight-to-wet-weight conversion factors (Ruzicka et al., 2016 [33]; see supplemental code).

Additional data on pelagic amphipods, ctenophores, small medusae, and large jellies from the Pre-recruit survey (2014 – 2019) were used to calculate average biomass density values (along with the JSOES data) for all transects that fell within overlapping subregions. The Pre-recruit survey (2017-2018) data were also used to parameterize pyrosome biomass. Pre-recruit data were provided as counts per trawl with corresponding length data for a subset of up to 30 specimens per trawl. Counts per trawl were converted to biomass densities by first converting average lengths (or bell diameter; provided by survey) to average weight with standard species-specific length-weight relationships [52](see "CountsToBiomass.R" in supplemental data and code) and then multiplying by counts to get total biomass (for each species) from each trawl. Biomass was converted to density by dividing by the volume of water sampled during each trawl.

Krill and shrimp

Areal krill biomass densities (mt km^{-2}) were provided by the hake survey (2015, 2017, and 2019; see Appendix for survey description). Because krill biomass estimates from the hake survey are not resolved to species level (due to the overlap in the frequency response of *E. pacifica* and *T. spinifera*), we used krill species data from the Pre-recruit survey (2019) along with the Newport Hydrographic Line (2014-2016) to apportion krill biomass from the hake survey into two functional groups (*Thysanoessa spinifera* and *Euphausia pacifica*; Table 2) based on the average relative proportion of each species observed (see "KrillBreakout.csv" in supplemental data and

code). We used data from the Pre-recruit survey (2014-2019) to parameterize biomass for pink shrimp (*Pandalus* spp.) and other pelagic shrimp (Sergestidae, Penaeidae), which were provided as counts and lengths and converted to biomass following the description under the "Zooplankton" subheading.

Juvenile fish

We used data from the Pre-recruit survey (2014-2019) to parameterize biomass for all juvenile fish groups (except salmonids; see below), which were provided as counts and lengths and converted to biomass following the description under the "Zooplankton" subheading above. Individual species data were then summed within functional groups as total group biomass densities (Table 1, 2; see "Biomass_Aggregation/" in Zenodo repository).

Coastal pelagic fish

Data for Pacific sardine, Pacific herring, Pacific chub mackerel, Pacific jack mackerel, and northern anchovy were provided by the SWFSC coastal pelagic species acoustic-trawl survey [53,54] as biomass densities (in mt/km^2; from 2015-2019; see Appendix).

Salmonids

We used 2014 – 2019 data from the JSOES to parameterize juvenile salmonids into eight distinct functional groups and adult salmonids into three groups based on species and life history characteristics (Table 2). The EcoTran platform does not currently support linked life stages, so juvenile salmonid groups do not recruit into adult salmonid groups. Juvenile coho salmon comprise their own group, juvenile Chinook salmon were split into six groups based on life

history and ocean entry timing (see below), and all other juvenile salmonids species that individually constitute a small percent of the total catch (<5%; e.g., steelhead, sockeye, chum) made up the final juvenile salmonid functional group (Table 2). Juvenile Chinook salmon were distinguished as spring versus fall run-type Chinook salmon based on genetic stock information [55,56] and broken out by life history (i.e., sub-yearlings and yearlings; based on fork-length and time of year; [57]), and ocean entry timing (i.e., May/June and September; [56,58]), which influences their migration behaviors and residence time in the NCC (and thus their trophic interactions with other functional groups). JSOES data on salmonids were provided as counts per trawl with length and weight information for individuals. Counts were multiplied by weight to get a biomass value for each trawl and then divided by the total volume sampled to calculate biomass density (mt km^{-3}) values for each functional group.

Hake

Areal biomass densities (mt km^{-2}) were provided (2015, 2017, and 2019) for age 2+ hake from the Pacific Hake Ecosystem Acoustic Trawl Survey [59,60]. Juvenile hake were provided by the Pre-recruit survey (2014-2019) as counts and lengths and converted to biomass following the description under the "Zooplankton" subheading above. Calculated biomass densities (within each model subregion) from the hake survey and Pre-recruit survey were then summed.

Groundfish and crabs

On 28 July 2021, we accessed the groundfish survey (see Appendix) database via the R package `nwfscSurvey` [61] and downloaded data from 2014-2019 on demersal species of interest (Table 2, S1). Data were provided as areal biomass densities (kg km^{-2}), which were divided by 1000 to

466 convert to consistent units for the model (mt km^{-2}). Individual species data were then summed
467 within functional groups as total group biomass densities (Table 1, 2).
468
469 *Seabirds*
470 We used seabird species data from JSOES during 2015-2019 to parameterize this model. Data
471 were provided as count densities, in individuals per square kilometer, and were converted to
472 biomass densities by multiplying by the average weight of individual birds, which were obtained
473 from the Sibley Guide to Birds [62] and the Cornell Lab of Ornithology's All About Birds
474 webpage [63]. Individual species data were then summed within functional groups as total group
475 biomass densities (Table 1, 2).
476
477 *Marine mammals*
478 Coastwide or stock-specific marine mammal biomasses were obtained from stock assessments
479 [64,65] and were used to scale regional biomass values calculated in a previous Northern
480 California Current ecosystem model [32,33]. In cases where population stock assessments have
481 not been updated, or populations have not drastically changed, the values were used directly
482 from the previous ecosystem model.
483
484 *Model-estimated groups*
485 While biomass for most groups was estimated with data, there were a few groups for which we
486 lacked survey data. Additionally, in a couple of cases where we did have some data, surveys
487 were inadequate samplers for particular functional groups (see below) – we instead either
488 allowed the model to estimate biomass by fixing Ecotrophic Efficiency (EE) values (0.85-0.9;

489 see Table 1 for a list of model-estimated groups) or by using biomass values from the previous
490 NCC ecosystem model [32,33]. Ecotrophic Efficiency values describe the proportion of a
491 functional group's production that is used by higher trophic levels (see 'Mass balancing' above).
492
493 Two groups sampled by the groundfish survey (see Appendix for survey descriptions) were
494 estimated by the model – the mesopelagic fish aggregate was likely above (in the water column)
495 the bottom-trawl net, and the miscellaneous small benthic fishes were likely too small and
496 avoidant to be adequately sampled by the survey. Epibenthic shrimp (Caridea) were similarly not
497 well sampled by the Pre-recruit survey, which relies on a nighttime midwater net trawl that
498 uncommonly captures small shrimp in the benthos; thus, this group was also estimated by the
499 model. Two groups of medium pelagic fish (smelt and saury) were not well sampled by the
500 JSOES, so we relied on biomass estimates from a previous NCC model [33]. Similarly, market
501 squid are caught by the Pre-recruit survey and JSOES, but neither survey provides an adequate
502 absolute estimate of biomass. These cases were not surprising as none of the listed groups were
503 designed to be sampled by the respective surveys. Some benthic groups (such as bivalves;
504 echinoderms; and other carnivorous epifauna such as small crabs, sea stars, and gastropods) have
505 not been well-sampled recently [66,67]. The remaining groups are not sampled (to our
506 knowledge) by any survey and were estimated by the model: juvenile chondrichthyes and other
507 benthic groups (mysids; suspension feeders such as barnacles, bryozoans, and sea anemones;
508 benthic amphipods, isopods, and cumaceans).
509

Diet matrix

The diet matrix partitions each predator's consumption rate amongst its prey (Fig 5). Together with the biomass densities informed in the model and the other trophic flow parameters [also referred to as physiology parameters (e.g., P/B, C/B, etc.); see Equation 2, Table 1], it expresses the biomass flows among functional groups (Fig 6, 7).

Diets were compiled as follows (see "DietWork/" in supplementary code). For each data source, unidentified material was removed from analyses, and observations were summed (across all individuals) by weight of prey (or % frequency of occurrence (FO) for marine mammals and kelp greenling) and then divided by the total weight (or % FO) of identified prey that was consumed to get a relative (standardized) proportion of each prey in the diet for a given predator species.

If multiple sources were used for one predator species, the resulting predator species' diet was computed as an average of diets calculated from each source, weighting the latter by the sample size (number of predator individuals) within each source. Then predators within the same functional group were combined, with each predator species contributing to a given functional group relative to (or weighted by) the proportion of biomass that a given species contributed to said functional group. For example, northern fur seals and harbor seals make up one functional group (small pinnipeds), but harbor seals account for 98.9% of the small pinniped functional group biomass in our model, whereas northern fur seals only account for 1.1%. Thus, the small pinniped functional group diet consists of harbor seal diet proportions multiplied by 0.989 and northern fur seal diets multiplied by 0.011 summed together.

If a prey grouping from a source was broader than our functional groups (e.g., “cephalopod” includes squid and octopuses, which are in separate functional groups in EcoTran), the relative proportion of prey going into each group was allocated proportionally to the biomass of the groups if they have been observed at least once in the diet of the predator. This procedure assumes that the more abundant prey are more readily available for consumption [31] (see “Build_Diet_Matrix.R” in supplemental data and code).

Diet information was obtained from local NCC studies to the extent possible. Data from small pinnipeds (Northern fur seals and some harbor seal diets), sharks (blue shark, common thresher shark, shortfin mako shark), Pacific spiny dogfish, California market squid, Northern anchovy, Pacific herring, Pacific jack mackerel, Pacific chub mackerel, Pacific sardine, Pacific saury, sablefish and hexagrammids (kelp greenling and lingcod) were taken from the California Current Trophic Database (hereafter ‘trophic database’; https://oceanview.pfeg.noaa.gov/cctd/; see ‘Diet sources’ in the Appendix). Other harbor seal diets [68,69] and other Pacific spiny dogfish diets [70] came from the literature and were combined with data from the trophic database as described above. In addition, for all groups mentioned above, diets obtained from the trophic database and the literature were arithmetically averaged with an early version of the food web of Ruzicka et al. (2012) [32]. The inclusion of more sources of information helps ensure that diets (which are always a product of imperfect sampling in time and space) are as diverse as possible, which more likely reflects the possibility that predators are consuming a diverse prey field, depending on what is available to them.

Juvenile salmonid diet data comes from the JSOES, which contains genetic stock information [71], and allows the diets to be broken out by specific functional groups (see "Juvenile salmon diets" in the Appendix and Table 2). Diet data for jellyfish, zooplankton, invertebrates, seabirds, cetaceans, and many fish groups were taken from an early version of the NCC food web [32]. See the Appendix for more information and Table S1 for a complete list of data sources for each functional group.

Marine mammal diets

In addition to the trophic database (https://oceanview.pfeg.noaa.gov/cctd/), harbor seal diets were extracted from the literature [68,69]. We followed Ruzicka et al. (2012) [32] in the use of Wright et al. (2007) [69] to parameterize harbor seal diets for their ecosystem model. That is, the proportion of salmon in harbor seal diets was scaled down from 36% to 20% to account for greater consumption of salmonids by river seals than by their coastwide counterparts, which are included in the model. To use river seal diets for the entire coast would greatly overestimate the total abundance of salmon consumed by harbor seals. As discussed above, resulting harbor seal diets were a weighted (by sample size) average of these three sources, with 94% of harbor seal diet data coming from the trophic database, which means Wright et al. (2007) does not strongly influence the overall model but remains important in order to represent a broader range of functional groups in harbor seal diets. California and Steller's sea lion diet data were taken from the literature [68,72,73] (see "MarineMammalDiets.R" in supplemental data and code), as were diet data from Northern elephant seals [74], and Southern resident killer whales [21].

578 ## Fisheries landings

579 Many of the larger commercial fisheries were updated (data from 2014-2021) directly from the
580 Pacific Coast Fisheries Information Network (PacFIN; http://pacfin.psmfc.org/; accessed 16
581 March 2022) for the following functional groups (see Table 2 for scientific names): the small
582 cephalopod aggregate, smelt aggregate, shad, sardine, herring, anchovy, coho salmon, Chinook
583 salmon, other salmon aggregate, jack mackerel, Pacific chub mackerel, hake, sablefish,
584 Hexagrammidae (lingcod, greenlings), and Gadidae (cod, haddock, walleye pollock). Smaller
585 commercial fisheries not mentioned above and recreational fisheries take were borrowed from a
586 previous NCC ecosystem model [32,33], which also obtained the data from PacFIN as well as the
587 Pacific States Marine Recreational Fisheries Information Network (RecFIN;
588 http://www.recfin.org/).
589
590 Fisheries landings in the PacFIN database were provided in large spatial domains that did not
591 perfectly correspond to our model subregions (Fig 1). Thus, we redistributed the fisheries
592 landings north-south to match our model subregions by scaling to the proportion of overlap in
593 latitude between PacFIN and EcoTran (see "PACFIN/" in supplemental data and code). Then, to
594 allocate landings across the shelf (i.e., bathymetric breaks; Fig 1), we considered that fisheries
595 landings were roughly proportional to where the species occurred in the ocean (reasonable
596 assumption since our model domains do not represent costly or intractable harvesting areas). We
597 used species distribution models for commercial forage fish (i.e., sardine, herring, anchovy, jack
598 mackerel, Pacific chub mackerel, and market squid; Barbara Muhling, *personal communication*),
599 fisheries bycatch information for adult salmon [75], the acoustic-trawl survey for hake, species
600 count data from the groundfish survey, and assumptions for other groups (e.g., bivalves were

601 taken in the nearshore region; see "PACFIN" in supplemental data and code). Fisheries landings
602 data by gear (also from PacFIN) were then used to proportionally allocate model subregion
603 landings to individual fishery fleets, which are tracked separately in EcoTran (Table 2, S4).
604 Discard rates were borrowed from a previous NCC food web (Table S5) [32,40,76].
605

606 ## Tuning detritus recycling

607 Rates of detritus recycling were tuned following Ruzicka et al. (2018) [40] so that the average
608 total primary production rate across the whole shelf and the ratio of new production to total
609 production [f-ratio = NO_3 uptake/(NO_3+NH_4 uptake)] of the model system were comparable to
610 independently obtained estimates. The f-ratio was tuned to approximate a cross-shelf range of
611 0.3 – 0.8 [77]. Total primary production was evaluated against the satellite-derived vertically
612 generalized production model (VGPM) [49].

613 Pelagic detritus and benthic detritus are recycled in the model via bacterial remineralization and
614 by direct consumption by metazoan consumers. The two major pathways of production loss from
615 the EcoTran model are through advective transport of nutrients, plankton, and detritus offshore
616 and through the sequestration of benthic detritus (Fig 2). Three recycling parameters, rates of
617 pelagic and benthic detritus remineralization and rates of benthic detritus sequestration, were
618 systematically varied in 0.1 unit increments from 0 to 1 for all possible parameter combinations
619 in 20-year simulation runs. Tuning simulations were visualized as f-ratio and total primary
620 productivity surface plots of two parameters at a time (see "Tuning_Detritus_Parameters/" in
621 supplement). We also assessed the number of functional groups whose production rates fell
622 below 1% of their original values at any point in the simulation – i.e., are going extinct in the
623 model [30].

We chose the detritus remineralization and sequestration values that generated f-ratios and total primary productivity values closest to realistic values while preventing functional groups going extinct. With benthic detritus sequestration rates above 0.2 (>20% of benthic detritus production becomes "lost" to the system at every time step), production rates of many groups were falling to unreasonably low values as too much detritus production was being eliminated from the system to support detritivory. We set benthic detritus sequestration at 0.1. Once the benthic detritus sequestration rate was fixed to 0.1, changes to pelagic and benthic detritus remineralization did not substantially change the f-ratio, primary productivity, or extinction rates (see "Tuning_Detritus_Parameters/" in supplemental data and code). Pelagic and benthic detritus remineralization were each set to 0.1 (see results).

Further model details can be found in previous EcoTran articles [27,32–34,76]. To be more open, reliable, transparent, and reproducible [79], we have provided data and code to reproduce and use this ecosystem model at https://doi.org/10.5281/zenodo.7079777.

Model validation

We used the mass-balancing steps described above [25,31], as well as the model validation diagnostics (described in Link, 2010 [39]), to visualize and assess the pre- and post-balance aggregated model to assess the plausibility of the food web parameterization. Food web evaluation criteria guidance from Link (2010) states that biomass density values of all functional groups should span 5 – 7 orders of magnitude, there should be a 5 – 10% decrease in biomass density (on the log scale) for every unit increase in trophic level, biomass-specific production values (P/B) should never exceed biomass-specific consumption (C/B) values, and ecotrophic efficiency (EE) for each group should be below 1 [39].

Within the coupled physical-biological model system, we assessed the persistence of functional groups over 100-year time dynamic simulations within the aggregated regional model. Within such short timeframes, functional groups should not go extinct when driven by a constant upwelling time series [30]. We drove a 100-year simulation with multiple constant (daily values repeated for each day of the year) upwelling time series. To assess the model dynamics under assumptions of stabile nutrient inputs, we drove the model under a range of constant upwelling conditions: the mean CUTI (~0.41; averaged across all years: 1988-2021, days: 1-366, and latitudes: 41-48°N; [41]), 10% of the mean CUTI (~0.04), and 2.5% of the mean CUTI (0.01). These arbitrary values were selected such that production values spanned a large range. We also ran a 100-year simulation with an average upwelling (CUTI) time series, which was averaged across 1988 - 2021 for each day of the year and repeated in each 100 years of the simulation. This average upwelling time series ensures that interannual variation is not adding unnecessary noise to our assessment of model stability and equilibrium (Fig S1).

We assessed whether or not the ecosystem model reached equilibrium states in such dynamic simulations by assessing extinction rates and population dynamic trends in the final 20 years of the 100-year, constant-upwelling simulation, as suggested by Kaplan and Marshall (2016) [30]. That is, biomass values for most groups should not change significantly in the last 20 years of the simulation. We visualized the functional group trends within the simulation to assess how many groups were changing by more than 5% in the last 20 years.

Lastly, we visualized time series outputs of primary production generated from our ecosystem model with independently-derived time series (2002-2021) of primary production estimates aggregated across our entire spatial domain [48,49]. This process allows us to assess whether the ecosystem model, driven by an upwelling time series (1988-2021 CUTI; [41]), can track the actual direction of change that we see in the ocean over short (i.e., daily) timescales.

Results

Our constructed EcoTran model was consistent with ecological energetics, as suggested by the "PREBAL" criteria of Link [39]. Biomass densities span 6 orders of magnitude (within the 5 – 7 suggested range; Fig 4) and the slope on the log scale is about an 8.5% change each trophic level [between the 5 – 10% suggested range [39]; see Fig 4B]. Biomass-specific production values (P/B) never exceed biomass-specific consumption (C/B) values, and ecotrophic efficiency (EE) values are all below 1 (Table 1). In general, P/B and C/B should decrease as trophic level (TL) increases, except homeotherms should be lower (for P/B) and higher (for C/B) than expected for other groups [39]. The model presented here appears to be consistent with this criteria (Fig 8), as a few deviations (or exceptions) are not a cause for concern [39]. Biomass estimates of primary productivity are on the same order as biomass estimates for detritus (Table 1; Fig 4B), which is also a sign that model parameterization is not unreasonable [39].

Some groups are consumed at relatively low levels (low EE values in Table 1 correspond roughly to the proportion consumed). Some notable groups are small copepods, with less than half of their substantial biomass (~26 mt/km^2) consumed (EE = 0.419); jack mackerel (~21 mt/km^2; only consumed at ~10% of potential, EE = 0.1); pyrosomes, which are nearly as dense

692 (~16 mt/km^2) but are hardly consumed at all (EE = 0.001); and three groups of jellies, none of
693 which are as dense (1.7, 0.05, and 0.1 mt/km^2) but are similarly unconsumed (EE = 0.02, 0.02,
694 and 0.08 respectively; Table 1).
695
696 Over a 100-year simulation, driven by constant time series and an average upwelling time series,
697 zero functional groups go extinct from the model (Fig 9, Fig S2). Of 83 living consumer groups,
698 only two groups changed by more than 5% in the final 20 years, and these are both long-lived
699 killer whale groups that are expected to have very slow population dynamics (red lines in Fig 9,
700 Fig S2; Table S6). The remaining groups appear to have reached a mostly stable equilibrium.
701
702 The f-ratio [NO_3 uptake/(NO_3+NH_4 uptake)] inner shelf is 0.68, mid shelf is 0.52, and outer shelf
703 is 0.43, which are reasonably comparable to the cross-shelf range and pattern (0.3 – 0.8) for the
704 NCC [77] and near values (0.75) previously used in NCC ecosystem models [40]. Total primary
705 productivity averaged across the ecosystem model is 3.25 mmol N m^{-3} d^{-1}, which is reasonably
706 close to the 1.99 mmol N m^{-3} d^{-1} VGPM estimate from satellite data [48] (see supplement,
707 "Fratio_PP_check.m"). Our model output matches the seasonal timing observed in a
708 phytoplankton primary productivity time series estimated from a vertically generalized
709 production model (VGPM; 2002 - 2021; Fig 10) [48,49].
710

711 ## Discussion

712 Here we have presented an end-to-end ecosystem model of the Northern California Current
713 marine ecosystem. Our model was built using many long-term West Coast ocean surveys [46],
714 databases, and literature and updates previous ecosystem models of the region [32,33,44,80]. The

ecosystem model is in thermodynamic balance, meaning that no functional groups produce more than they consume, and model validation suggests that our model parameterization is energetically feasible [39].

In time-dynamic simulations, no functional groups go extinct and functional group biomasses are stable after 100-year simulations (Fig 9, Fig S2), suggesting that the model is stable and reasonably parameterized [30]. Our upwelling-driven ecosystem model-derived estimates of primary production tracks the satellite imagery-derived production model estimates of primary productivity (Fig 10) [48,49]. Primary productivity in the ecosystem model is determined by nutrient inputs to the system which are driven by the coastal upwelling transport index (CUTI; Fig S1) [41], and the remarkably close cyclical resemblance to the VGPM time series is an indication that the ecosystem model is capturing the appropriate primary productivity dynamics well-enough to reproduce such dynamics (Fig 10). This last model validation check is promising, as primary production is what determines the bottom-up energy flux to higher trophic levels and drives the production of the entire food web (Fig 7).

Our model is also congruent with model guidelines that are based on an understanding of trophic ecology [39]. Some seabirds (groups 71 – 76) fall below the log scale biomass density – trophic level line (Fig 4B), which may indicate that biomass densities for some of these higher trophic levels are actually under-estimated (inadequacy of the onboard observations for assessing abundance), which may be possible if some seabirds actively avoid survey vessels. Perhaps a more likely explanation is that each of these groups are more taxonomically resolved compared to other groups in the model (Table 1, 2). When these groups are combined for visualization

(purple point in Fig 4B), they fall much closer to the trend line. Thus, it is worth noting that the choice of functional group aggregation can impact the interpretation of some of these validation diagnostics, but it does not mean that this will influence the model or that they should necessarily be combined. Combining all seabirds into one functional group would severely muddy our ability to understand any individual group's impact on the ecosystem, if that ability were of scientific interest.

Some groups in our model appear to be bottom-up energetic pathway 'dead-ends' in that they are not consumed nearly as much as they could be. Small copepods for example appear to be able to handle double the predation that they currently do (see calculated EE). It seems unlikely that this functional group is so abundant that it swamps predators, since euphausiids are both more available and more consumed than the small copepod group. It is possible, however, that diets of copepod predators are not described well enough to parameterize the real consumption of this group. The size distinction between small and large copepods here is captured in the surveys that sample them, but this level of detail is often lost in diet analyses, especially due to breakdown during digestion (which may lead to an underestimation of consumed invertebrates in general). Here, we assume predators with copepods in their diets consumed these two groups based on the relative abundance of each. If small copepods are actually consumed more, we may be underestimating their contribution to the next trophic level.

Jack mackerel are under-consumed in the system. This species is currently more abundant in this system than they have been in the past 10 years [54], but it is not typically a species targeted by US fisheries, and fisheries catch reported by PacFIN is relatively low. The diets of some

761 potential pelagic predators, such as sharks, tunas, and toothed whales, are somewhat limited in
762 space and time. These pelagic predators likely overlap more strongly with the pelagic
763 distribution of jack mackerel than other predators in the model, which means we may be
764 underestimating the consumption of jack mackerel by predators. Additionally, it is possible that
765 marine mammal diet studies that report "unidentified bony fish" due to the difficulty of
766 identifying hard parts might be causing us to underestimate the total predation on jack mackerel.
767 It is also possible that jack mackerel biomass is overestimated in the ecosystem, but this does not
768 seem like an adequate explanation to fully account for the lack of consumption of the group.
769 While this requires further research, this may be a relatively under-exploited group that
770 commercial fisheries have yet to exploit.
771
772 Other energetic dead-ends such as the gelatinous zooplankton: jellies and pyrosomes are not
773 surprising given the low energy content of such prey. However, jellies and other soft-bodied
774 organisms are often so easily digested that they are often underrepresented in laboratory-based
775 visual diet analyses [81]. Alternative methods, such as DNA analysis, stable isotopes, and
776 animal-borne cameras, suggest that gelatinous zooplankton are consumed far more than we used
777 to think [82,83], which means we likely underestimate their role in transferring energy to higher
778 trophic levels here.
779
780 Our hope is that the model presented here can aid in making management decisions surrounding
781 the sustainable use of our oceans and the fate of imperiled species. We have, for example,
782 expanded the functional groups within previous versions of the model to include endangered
783 species act (ESA)-listed populations such as southern resident killer whales and their preferred

prey, Chinook salmon [21]. Pacific salmon (*Oncorhynchus* spp.) are a group of general interest within the NCC due to their economic [84,85], ecological [86–89], and cultural [90–93] benefits and their large scale declines across much of their range [94,95]. Some populations of Chinook salmon (*O. tshawytscha*) are listed as threatened or endangered [96] while others continue to be commercially and recreationally fished [97,98]. The most vulnerable life stage of the Chinook salmon is thought to be when salmon smolts enter the ocean and begin growing and transitioning into adults [99–103]. However, it is notoriously difficult to assess what occurs in the ocean because sampling is spatially and temporally incomplete and the food web is large, complex, and understudied. Here we expand subyearling and yearling Chinook salmon from the previous NCC EcoTran model into six functional groups (see Table 2), which will allow future work to understand the role that the ocean stage plays in juvenile Chinook salmon persistence.

While our model presented here contains 90 functional groups, there are notable groups that are not well-parameterized and/or are missing from the model entirely. Many of the benthic organisms have not recently been sampled in any surveys that we are aware of. Yet, benthic groups are likely important to the ecosystem as they comprise a large portion of the total biomass (Table 1; Fig 4) and recycle nutrients by consuming benthic detritus (Fig 5, 6) [32,80]. Marine mammal biomass estimates are based solely on coastwide or stock-specific marine mammal population assessments, some of which have not been recently updated due to the stability of such populations or the absence of substantial threats to those species [64]. While these biomass estimates appear well within reason (Fig 4), more recent and spatially-resolved marine mammal data would reduce our uncertainty in these values. Additionally, many of the marine mammal and seabird groups, other than pinnipeds, lack thorough (i.e., in time, space, and sampling effort)

diet analyses. An increased sampling effort would be valuable given the unknown importance of some understudied groups as predators (e.g., harbor porpoises on endangered salmon) [104,105].

Some groups have been omitted from the model. One example, kelp, is known to be a crucial component of this ecosystem [106], as kelp forests provide habitat and food for various species of fish, including commercially important species and those listed under the Endangered Species Act, such as populations of Pacific salmon [107–110]. Others such as abalone and urchins are lumped into very general functional groups, where a lack of available empirical data has forced a reliance on allowing our ecosystem model to estimate total biomass. The California Current is currently experiencing urchin barrens where kelp forests once existed [111–113]. Recent marine heatwaves in combination with booming populations of urchins has taken such a toll on red abalone that Northern California and Oregon recreational fisheries (N. CA fishery valued at \$44M year^{-1}) have been completely closed [112,114]. As increased attention is placed on the importance of ecosystem-based fisheries management, more data on these understudied functional groups will likely become available. The ecosystem model presented here would be a useful framework with which to assess various future scenarios and management strategies pertaining to such important functional groups.

Our model comprises a highly interconnected, albeit simplified, view of the Northern California Current ecosystem and provides a flexible framework for understanding complex food web dynamics, management actions, and future states such as various climate change futures. The EcoTran ecosystem modeling framework can be used to estimate the pressure that various consumer groups exert on lower trophic levels and the rest of the ecosystem, identify important

food web nodes and how energy is transferred between them, compare ecosystem states during periods of low and high predator or competitor biomass, and to conduct simulation analyses to estimate the impact of events such as northward expansions of fish, jellyfish blooms, fishing pressure, climate change, and other events upon the ecosystem [32,32–34,77,115]. It is important to note, however, that this view is based on an incomplete snapshot in time and space based on limited available data. Ecosystem modeling efforts would benefit from additional surveys and, importantly, more readily available data [79] as is being done more effectively in the southern extent of the California Current [https://calcofi.org/data/]. As we move beyond single-species models towards holistic ecosystem-based fisheries management, we must openly and collaboratively integrate our disparate datasets and collective knowledge to solve the intricate problems we currently face in a changing world.

Data availability statement

Ecosystem model files and scripts, including the balanced and unbalanced diet matrices, biomass estimates, various cleaning scripts, readme files, and all files mentioned in the text can be found at https://doi.org/10.5281/zenodo.7079777.

Acknowledgements

We thank Isaac Kaplan for many conversations about survey data, ecosystem modeling, and model validation; Isaac Kaplan and Brian Wells for reviewing an earlier version of this manuscript; Douglas Draper for information on the proportion of pyrosomes in the diets of several bottomfish; Anne Thompson for data on pyrosome diets; Sheanna Steingass and Casey Clark for sharing their knowledge of pinnipeds with us; Barbara Muhling for sharing her species

distribution models for coastal pelagic species and market squid with us; Kevin Stierhoff for sharing the coastal pelagic species survey data with us; and Chantel Wetzel and her collaborators for creating a user-friendly R package to download West Coast Groundfish survey data from.

References

1. Checkley Jr DM, Barth JA. Patterns and processes in the California Current System. Progress in Oceanography. 2009;83: 49–64.

2. Kaplan IC, Leonard J. From krill to convenience stores: forecasting the economic and ecological effects of fisheries management on the US West Coast. Marine Policy. 2012;36: 947–954.

3. Weber ED, Auth TD, Baumann-Pickering S, Baumgartner TR, Bjorkstedt EP, Bograd SJ, et al. State of the California current 2019–2020: Back to the future with marine heatwaves? Frontiers in Marine Science. 2021; 1081.

4. Chan F, Barth JA, Lubchenco J, Kirincich A, Weeks H, Peterson WT, et al. Emergence of anoxia in the California current large marine ecosystem. Science. 2008;319: 920–920.

5. Peterson JO, Morgan CA, Peterson WT, Lorenzo ED. Seasonal and interannual variation in the extent of hypoxia in the northern California Current from 1998–2012. Limnology and Oceanography. 2013;58: 2279–2292.

6. Chan F, Barth JA, Blanchette CA, Byrne RH, Chavez F, Cheriton O, et al. Persistent spatial structuring of coastal ocean acidification in the California Current System. Scientific Reports. 2017;7: 1–7.

7. Marshall KN, Kaplan IC, Hodgson EE, Hermann A, Busch DS, McElhany P, et al. Risks of ocean acidification in the California Current food web and fisheries: ecosystem model projections. Global Change Biology. 2017;23: 1525–1539.

8. Bond NA, Cronin MF, Freeland H, Mantua N. Causes and impacts of the 2014 warm anomaly in the NE Pacific. Geophysical Research Letters. 2015;42: 3414–3420.

9. Leising AW, Schroeder ID, Bograd SJ, Abell J, Durazo R, Gaxiola-Castro G, et al. State of the California Current 2014-15: Impacts of the Warm-Water" Blob". California Cooperative Oceanic Fisheries Investigations Reports. 2015;56.

10. Amaya DJ, Miller AJ, Xie S-P, Kosaka Y. Physical drivers of the summer 2019 North Pacific marine heatwave. Nature communications. 2020;11: 1–9.

11. McCabe RM, Hickey BM, Kudela RM, Lefebvre KA, Adams NG, Bill BD, et al. An unprecedented coastwide toxic algal bloom linked to anomalous ocean conditions. Geophysical Research Letters. 2016;43: 10–366.

12. Moore SK, Dreyer SJ, Ekstrom JA, Moore K, Norman K, Klinger T, et al. Harmful algal blooms and coastal communities: Socioeconomic impacts and actions taken to cope with the 2015 US West Coast domoic acid event. Harmful algae. 2020;96: 101799.

13. Peterson WT, Fisher JL, Strub PT, Du X, Risien C, Peterson J, et al. The pelagic ecosystem in the Northern California Current off Oregon during the 2014–2016 warm anomalies within the context of the past 20 years. Journal of Geophysical Research: Oceans. 2017;122: 7267–7290.

14. Wells BK, Schroeder ID, Bograd SJ, Hazen EL, Jacox MG, Leising A, et al. State of the California Current 2016-17: still anything but" normal" in the north. California Cooperative Oceanic Fisheries Investigations Reports. 2017;58: 1–55.

15. Morgan CA, Beckman BR, Weitkamp LA, Fresh KL. Recent ecosystem disturbance in the Northern California current. Fisheries. 2019;44: 465–474.

16. Harvey CJ, Garfield NT, Williams GD, Tolimieri N. Ecosystem Status Report of the California Current for 2020-21: A Summary of Ecosystem Indicators Compiled by the California Current Integrated Ecosystem Assessment Team (CCIEA). 2021.

17. Frölicher TL, Laufkötter C. Emerging risks from marine heat waves. Nature communications. 2018;9: 1–4.

18. Pozo Buil M, Jacox MG, Fiechter J, Alexander MA, Bograd SJ, Curchitser EN, et al. A dynamically downscaled ensemble of future projections for the California current system. Frontiers in Marine Science. 2021;8: 612874.

19. Crozier LG, McClure MM, Beechie T, Bograd SJ, Boughton DA, Carr M, et al. Climate vulnerability assessment for Pacific salmon and steelhead in the California Current Large Marine Ecosystem. PloS one. 2019;14: e0217711.

20. Crozier LG, Burke BJ, Chasco BE, Widener DL, Zabel RW. Climate change threatens Chinook salmon throughout their life cycle. Communications biology. 2021;4: 1–14.

21. Hanson MB, Emmons CK, Ford MJ, Everett M, Parsons K, Park LK, et al. Endangered predators and endangered prey: Seasonal diet of Southern Resident killer whales. PloS one. 2021;16: e0247031.

22. Panel EPA. Ecosystem-based fishery management. National Marine Fisheries Service, Washington, DC. 1999.

23. Pikitch EK, Santora C, Babcock EA, Bakun A, Bonfil R, Conover DO, et al. Ecosystem-based fishery management. American Association for the Advancement of Science; 2004.

24. Link J. Ecosystem-based fisheries management: confronting tradeoffs. Cambridge University Press; 2010.

25. Christensen V, Walters CJ. Ecopath with Ecosim: methods, capabilities and limitations. Ecological modelling. 2004;172: 109–139.

26. Fulton EA, Link JS, Kaplan IC, Savina-Rolland M, Johnson P, Ainsworth C, et al. Lessons in modelling and management of marine ecosystems: the Atlantis experience. Fish and fisheries. 2011;12: 171–188.

27. Steele JH, Ruzicka JJ. Constructing end-to-end models using ECOPATH data. Journal of Marine Systems. 2011;87: 227–238.

28. Collie JS, Botsford LW, Hastings A, Kaplan IC, Largier JL, Livingston PA, et al. Ecosystem models for fisheries management: finding the sweet spot. Fish and Fisheries. 2016;17: 101–125.

29. Harvey CJ, Reum JC, Poe MR, Williams GD, Kim SJ. Using conceptual models and qualitative network models to advance integrative assessments of marine ecosystems. Coastal Management. 2016;44: 486–503.

30. Kaplan IC, Marshall KN. A guinea pig's tale: learning to review end-to-end marine ecosystem models for management applications. ICES Journal of Marine Science. 2016;73: 1715–1724.

31. Aydin KY, Gaichas SK, Ortiz I, Kinzey DH, Friday N. A comparison of the Bering Sea, Gulf of Alaska, and Aleutian Islands large marine ecosystems through food web modeling. 2007.

32. Ruzicka JJ, Brodeur RD, Emmett RL, Steele JH, Zamon JE, Morgan CA, et al. Interannual variability in the Northern California Current food web structure: changes in energy flow pathways and the role of forage fish, euphausiids, and jellyfish. Progress in Oceanography. 2012;102: 19–41.

33. Ruzicka JJ, Brink KH, Gifford DJ, Bahr F. A physically coupled end-to-end model platform for coastal ecosystems: Simulating the effects of climate change and changing upwelling characteristics on the Northern California Current ecosystem. Ecological Modelling. 2016;331: 86–99.

34. Ruzicka JJ, Daly EA, Brodeur RD. Evidence that summer jellyfish blooms impact Pacific Northwest salmon production. Ecosphere. 2016;7: e01324.

35. Chiaverano LM, Robinson KL, Tam J, Ruzicka JJ, Quiñones J, Aleksa KT, et al. Evaluating the role of large jellyfish and forage fishes as energy pathways, and their interplay with fisheries, in the Northern Humboldt Current System. Progress in Oceanography. 2018;164: 28–36.

36. Kaplan IC, Francis TB, Punt AE, Koehn LE, Curchitser E, Hurtado-Ferro F, et al. A multi-model approach to understanding the role of Pacific sardine in the California Current food web. Marine Ecology Progress Series. 2019;617: 307–321.

37. Bailey KM. Shifting control of recruitment of walleye pollock Theragra chalcogramma after a major climatic and ecosystem change. Marine Ecology Progress Series. 2000;198: 215–224.

38. Hunt Jr GL, Stabeno P, Walters G, Sinclair E, Brodeur RD, Napp JM, et al. Climate change and control of the southeastern Bering Sea pelagic ecosystem. Deep Sea Research Part II: Topical Studies in Oceanography. 2002;49: 5821–5853.

39. Link JS. Adding rigor to ecological network models by evaluating a set of pre-balance diagnostics: a plea for PREBAL. Ecological Modelling. 2010;221: 1580–1591.

40. Ruzicka JJ, Steele JH, Brink KH, Gifford DJ, Bahr F. Understanding large-scale energy flows through end-to-end shelf ecosystems-the importance of physical context. Journal of Marine Systems. 2018;187: 235–249.

41. Jacox MG, Edwards CA, Hazen EL, Bograd SJ. Coastal upwelling revisited: Ekman, Bakun, and improved upwelling indices for the US West Coast. Journal of Geophysical Research: Oceans. 2018;123: 7332–7350.

42. Peterson WT, Keister JE. Interannual variability in copepod community composition at a coastal station in the northern California Current: a multivariate approach. Deep Sea Research Part II: Topical Studies in Oceanography. 2003;50: 2499–2517.

43. Preikshot D. Data sources and derivation of parameters for generalised Northeast Pacific Ocean Ecopath with Ecosim models. UBC Fisheries Centre Research Reports. 2005;13: 179–206.

44. Field JC, Francis RC, Aydin K. Top-down modeling and bottom-up dynamics: linking a fisheries-based ecosystem model with climate hypotheses in the Northern California Current. Progress in Oceanography. 2006;68: 238–270.

45. Shenker JM. Carbon content of the neritic scyphomedusa Chrysaora fuscescens. Journal of Plankton Research. 1985;7: 169–173.

46. O'Loughlin JH, Bernard KS, Daly EA, Zeman S, Fisher JL, Brodeur RD, et al. Implications of Pyrosoma atlanticum range expansion on phytoplankton standing stocks in the Northern California Current. Progress in Oceanography. 2020;188: 102424.

47. Gallo ND, Bowlin NM, Thompson AR, Satterthwaite EV, Brady B, Semmens BX. Fisheries Surveys Are Essential Ocean Observing Programs in a Time of Global Change: A Synthesis of Oceanographic and Ecological Data From US West Coast Fisheries Surveys. 2022.

48. Pennington M. Estimating the mean and variance from highly skewed marine data. Fishery Bull. 1996;94: 498–505.

49. Behrenfeld MJ, Falkowski PG. Photosynthetic rates derived from satellite-based chlorophyll concentration. Limnology and oceanography. 1997;42: 1–20.

50. O'Reilly JE, Maritorena S, Siegel DA, O'Brien MC, Toole D, Mitchell BG, et al. Ocean color chlorophyll a algorithms for SeaWiFS, OC2, and OC4: Version 4. SeaWiFS postlaunch calibration and validation analyses, Part. 2000;3: 9–23.

51. Pebesma E, Bivand R, Pebesma ME, RColorBrewer S, Collate AAA. Package 'sp.' The Comprehensive R Archive Network. 2012.

52. Strickland J. Measuring the production of marine phytoplankton. Fish Res Bd Canada Bull. 1960;122.

53. Froese R, Pauly D. FishBase version (02/2022). 2022. Available: www.fishbase.org

54. Zwolinski JP, Demer DA, Cutter Jr GR, Stierhoff K, Macewicz BJ. Building on fisheries acoustics for marine ecosystem surveys. Oceanography. 2014;27: 68–79.

55. Stierhoff KL, Zwolinski JP, Demer DA. Distribution, Biomass, and Demography of Coastal Pelagic Fishes in the California Current Ecosystem During Summer 2019 Based on Acoustic-Trawl Sampling. US Department of Commerce, NOAA Technical Memorandum NMFS-SWFSC-626. 2020. doi:10.25923/nghv-7c40

56. Van Doornik DM, Teel DJ, Kuligowski DR, Morgan CA, Casillas E. Genetic analyses provide insight into the early ocean stock distribution and survival of juvenile coho salmon off the coasts of Washington and Oregon. North American Journal of Fisheries Management. 2007;27: 220–237.

57. Weitkamp LA, Teel DJ, Liermann M, Hinton SA, Van Doornik DM, Bentley PJ. Stock-specific size and timing at ocean entry of Columbia River juvenile Chinook salmon and steelhead: implications for early ocean growth. Marine and Coastal Fisheries. 2015;7: 515–534.

58. Fisher JP, Pearcy WG. Distribution and residence times of juvenile fall and spring chinook salmon in Coos Bay, Oregon. Fishery Bulletin. 1990;88: 51–58.

59. Teel DJ, Burke BJ, Kuligowski DR, Morgan CA, Van Doornik DM. Genetic identification of Chinook salmon: stock-specific distributions of juveniles along the Washington and Oregon coasts. Marine and Coastal Fisheries. 2015;7: 274–300.

60. Fleischer G, Cooke KD, Ressler PH, Thomas RE, De Blois SK, Hufnagle LC. The 2005 integrated acoustic and trawl survey of Pacific hake, Merluccius productus, in US and Canadian waters off the Pacific coast. 2008.

61. de Blois S. The 2019 Joint US–Canada Integrated Ecosystem and Pacific Hake Acoustic-Trawl Survey: Cruise Report SH-19-06. 2020.

62. Wetzel CR, Johnson KF, Hicks AC. nwfscSurvey: Northwest Fisheries Science Center Survey. R package version 20. 2021. Available: https://rdrr.io/github/nwfsc-assess/nwfscSurvey/

63. Sibley D. The Sibley guide to birds. National Audubon Society.; 2001.

64. Cornell Lab of Ornithology. All About Birds. Cornell Lab of Ornithology, Ithaca, New York. 2019 [cited 22 Sep 2021]. Available: https://www.allaboutbirds.org/

65. Carretta JV, Oleson EM, Forney K, Muto MM, Weller DW, Lang AR, et al. US Pacific Marine Mammal Stock Assessments: 2020. 2021.

66. Muto MM, Helker VT, Delean BJ, Young NC, Freed JC, Angliss RP, et al. Alaska marine mammal stock assessments, 2020. 2021.

67. Lie U. Standing crop of benthic infauna in Puget Sound and off the coast of Washington. Journal of the Fisheries Board of Canada. 1969;26: 55–62.

68. Carey Jr AG. Ecological observations on the benthic invertebrates from the central Oregon continental shelf. Oregon State Univ., Corvallis. Dept. of Oceanography; 1972.

69. Riemer SD, Brown RF. Pinniped Food Habits in Oregon. 1996.

70. Wright BE, Riemer SD, Brown RF, Ougzin AM, Bucklin KA. Assessment of harbor seal predation on adult salmonids in a Pacific Northwest estuary. Ecological Applications. 2007;17: 338–351.

71. Brodeur RD, Fleming IA, Bennett JM, Campbell MA. Summer distribution and feeding of spiny dogfish off the Washington and Oregon coasts. Biology and management of dogfish sharks Am Fish Soc, Bethesda, Maryland. 2009; 39–51.

72. Daly EA, Brodeur RD, Weitkamp LA. Ontogenetic shifts in diets of juvenile and subadult coho and Chinook salmon in coastal marine waters: important for marine survival? Transactions of the American Fisheries Society. 2009;138: 1420–1438.

73. Riemer SD, Wright BE, Brown RF. Food habits of Steller sea lions (Eumetopias jubatus) off Oregon and northern California, 1986–2007. 2011.

74. Akmajian AM, Scordino JJ, Acevedo-Gutiérrez A. Year-round algal toxin exposure in free-ranging sea lions. Marine Ecology Progress Series. 2017;583: 243–258.

75. Antonelis GA, Lowry MS, Fiscus CH, Stewart BS, Delong R. Diet of the northern elephant seal. Elephant Seals: Population Ecology, Behavior, and Physiology. University of California Press, Berkeley, California; 1994.

76. Richerson KE, Somers KA, Jannot JE, Tuttle VJ, Riley NB, McVeigh JT. Observed and Estimated Bycatch of Salmon in US West Coast Fisheries, 2002-20. 2022.

77. Ruzicka J, Brodeur RD, Cieciel K, Decker MB. Examining the ecological role of jellyfish in the Eastern Bering Sea. ICES Journal of Marine Science. 2020;77: 791–802.

78. Kokkinakis SA, Wheeler PA. Nitrogen uptake and phytoplankton growth in coastal upwelling regions. Limnology and Oceanography. 1987;32: 1112–1123.

79. Gomes DG, Pottier P, Crystal-Ornelas R, Hudgins EJ, Foroughirad V, Sánchez-Reyes LL, et al. Why don't we share data and code? Perceived barriers and benefits to public archiving practices. Proceedings of the Royal Society B. 2022;289: 20221113.

80. Field J, Francis R. Mass balance models of the Northern California Current. UBC Fisheries Centre Research Reports. 2005;13: 207–216.

81. Brodeur RD, Buckley TW, Lang GM, Draper DL, Buchanan JC, Hibpshman RE. Demersal fish predators of gelatinous zooplankton in the Northeast Pacific Ocean. Marine Ecology Progress Series. 2021;658: 89–104.

82. Doyle TK, Houghton JD, McDevitt R, Davenport J, Hays GC. The energy density of jellyfish: estimates from bomb-calorimetry and proximate-composition. Journal of Experimental Marine Biology and Ecology. 2007;343: 239–252.

83. Hays GC, Doyle TK, Houghton JD. A paradigm shift in the trophic importance of jellyfish? Trends in ecology & evolution. 2018;33: 874–884.

84. Knapp G, Guettabi M, Goldsmith OS. The economic importance of the Bristol Bay salmon industry. 2013.

85. Criddle KR, Shimizu I. The economic importance of wild Pacific salmon. Salmon: biology, ecological impacts and economic importance Nova Science Publishers. 2014; 269–306.

86. Gende SM, Edwards RT, Willson MF, Wipfli MS. Pacific salmon in aquatic and terrestrial ecosystems: Pacific salmon subsidize freshwater and terrestrial ecosystems through several pathways, which generates unique management and conservation issues but also provides valuable research opportunities. BioScience. 2002;52: 917–928.

87. Hilderbrand GV, Farley SD, Schwartz CC, Robbins CT. Importance of salmon to wildlife: implications for integrated management. Ursus. 2004;15: 1–9.

88. Verspoor JJ, Braun DC, Stubbs MM, Reynolds JD. Persistent ecological effects of a salmon-derived nutrient pulse on stream invertebrate communities. Ecosphere. 2011;2: 1–17.

89. Levi T, Hilderbrand GV, Hocking MD, Quinn TP, White KS, Adams MS, et al. Community ecology and conservation of bear-salmon ecosystems. Frontiers in Ecology and Evolution. 2020;8: 433.

90. Montgomery DR. King of fish: the thousand-year run of salmon. Westview Press; 2003.

91. Halffman CM, Potter BA, McKinney HJ, Finney BP, Rodrigues AT, Yang DY, et al. Early human use of anadromous salmon in North America at 11,500 y ago. Proceedings of the National Academy of Sciences. 2015;112: 12344–12348.

92. Adams MS, Connors B, Levi T, Shaw D, Walkus J, Rogers S, et al. Local Values and Data Empower Culturally Guided Ecosystem-Based Fisheries Management of the Wuikinuxv Bear–Salmon–Human System. Marine and Coastal Fisheries. 2021;13: 362–378.

93. Atlas WI, Ban NC, Moore JW, Tuohy AM, Greening S, Reid AJ, et al. Indigenous systems of management for culturally and ecologically resilient Pacific salmon (Oncorhynchus spp.) fisheries. BioScience. 2021;71: 186–204.

94. Nehlsen W, Williams JE, Lichatowich JA. Pacific salmon at the crossroads: stocks at risk from California, Oregon, Idaho, and Washington. Fisheries. 1991;16: 4–21.

95. Lichatowich JA. Salmon without rivers: a history of the Pacific salmon crisis. Island Press; 2001.

96. US Office of the Federal Register. Endangered and threatened wildlife; final rule to revise the Code of Federal Regulations for species under the jurisdiction of the National Marine Fisheries Service, final rule. Federal Register. 2014;71: 20802–20817.

97. Satterthwaite WH, Ciancio J, Crandall E, Palmer-Zwahlen ML, Grover AM, O'Farrell MR, et al. Stock composition and ocean spatial distribution inference from California recreational Chinook salmon fisheries using genetic stock identification. Fisheries Research. 2015;170: 166–178.

98. Shelton AO, Satterthwaite WH, Ward EJ, Feist BE, Burke B. Using hierarchical models to estimate stock-specific and seasonal variation in ocean distribution, survivorship, and aggregate abundance of fall run Chinook salmon. Canadian Journal of Fisheries and Aquatic Sciences. 2019;76: 95–108.

99. Holtby LB, Andersen BC, Kadowaki RK. Importance of smolt size and early ocean growth to interannual variability in marine survival of coho salmon (Oncorhynchus kisutch). Canadian Journal of Fisheries and Aquatic Sciences. 1990;47: 2181–2194.

100. Wells BK, Grimes CB, Sneva JG, McPherson S, Waldvogel JB. Relationships between oceanic conditions and growth of Chinook salmon (Oncorhynchus tshawytscha) from California, Washington, and Alaska, USA. Fisheries Oceanography. 2008;17: 101–125.

101. Wells BK, Santora JA, Schroeder ID, Mantua N, Sydeman WJ, Huff DD, et al. Marine ecosystem perspectives on Chinook salmon recruitment: a synthesis of empirical and modeling studies from a California upwelling system. Marine Ecology Progress Series. 2016;552: 271–284.

102. Wells BK, Santora JA, Henderson MJ, Warzybok P, Jahncke J, Bradley RW, et al. Environmental conditions and prey-switching by a seabird predator impact juvenile salmon survival. Journal of Marine Systems. 2017;174: 54–63.

103. Duffy EJ. Factors during early marine life that affect smolt-to-adult survival of ocean-type Puget Sound Chinook salmon (Oncorhynchus tshawytscha). University of Washington; 2009.

104. D'Alessandro DN, Duffield DA. Salmonid passive integrated transponder tags and coded wire tags found in the forestomach of a harbor porpoise (Phocoena phocoena) in southwestern Washington. Fishery Bulletin. 2019;117.

105. Elliser CR, Calambokidis J, D'Alessandro DN, Duffield DA, Huggins JL, Rice J, et al. Prey-related asphyxiation in harbor porpoises (Phocoena phocoena) along the US west coast: Importance of American shad (Alosa sapidissima) on adult female harbor porpoise mortality. Oceans. MDPI; 2020. p. 8.

106. Steneck RS, Graham MH, Bourque BJ, Corbett D, Erlandson JM, Estes JA, et al. Kelp forest ecosystems: biodiversity, stability, resilience and future. Environmental conservation. 2002;29: 436–459.

107. Carr MH. Effects of macroalgal dynamics on recruitment of a temperate reef fish. Ecology. 1994;75: 1320–1333.

108. National Marine Fisheries Service. Rockfish Recovery Plan: Puget Sound / Georgia Basin yelloweye rockfish (Sebastes ruberrimus) and bocaccio (Sebastes paucispinis). National Marine Fisheries Service. 2017.

109. Teagle H, Hawkins SJ, Moore PJ, Smale DA. The role of kelp species as biogenic habitat formers in coastal marine ecosystems. Journal of Experimental Marine Biology and Ecology. 2017;492: 81–98.

110. Shaffer JA, Munsch SH, Cordell JR. Kelp forest zooplankton, forage fishes, and juvenile salmonids of the northeast pacific nearshore. Marine and Coastal Fisheries. 2020;12: 4–20.

111. Lawrence JM. On the relationships between marine plants and sea urchins. Oceanogr Mar Biol Ann Rev. 1975;13: 213–286.

112. Rogers-Bennett L, Catton CA. Marine heat wave and multiple stressors tip bull kelp forest to sea urchin barrens. Scientific reports. 2019;9: 1–9.

113. Wernberg T, Krumhansl K, Filbee-Dexter K, Pedersen MF. Status and trends for the world's kelp forests. World seas: An environmental evaluation. Elsevier; 2019. pp. 57–78.

114. Reid J, Rogers-Bennett L, Vasquez F, Pace M, Catton CA, Kashiwada JV, et al. The economic value of the recreational red abalone fishery in northern California. 2016.

115. Auth TD, Daly EA, Brodeur RD, Fisher JL. Phenological and distributional shifts in ichthyoplankton associated with recent warming in the northeast Pacific Ocean. Global Change Biology. 2018;24: 259–272.

116. Chu D, Lawson GL, Wiebe PH. Estimation of biological parameters of marine organisms using linear and nonlinear acoustic scattering model-based inversion methods. The Journal of the Acoustical Society of America. 2016;139: 2885–2895.

117. Phillips EM, Chu D, Gauthier S, Parker-Stetter SL, Shelton AO, Thomas RE. Spatiotemporal variability of euphausiids in the California Current Ecosystem: insights from a recently developed time series. ICES Journal of Marine Science. 2022;79: 1312–1326.

118. Brodeur RD, Fisher JP, Emmett RL, Morgan CA, Casillas E. Species composition and community structure of pelagic nekton off Oregon and Washington under variable oceanographic conditions. Marine Ecology Progress Series. 2005;298: 41–57.

119. Peterson WT, Morgan CA, Fisher JP, Casillas E. Ocean distribution and habitat associations of yearling coho (Oncorhynchus kisutch) and Chinook (O. tshawytscha) salmon in the northern California Current. Fisheries Oceanography. 2010;19: 508–525.

120. Schabetsberger R, Morgan CA, Brodeur RD, Potts CL, Peterson WT, Emmett RL. Prey selectivity and diel feeding chronology of juvenile chinook (Oncorhynchus tshawytscha) and coho (O. kisutch) salmon in the Columbia River plume. Fisheries Oceanography. 2003;12: 523–540.

121. Morgan CA, De Robertis A, Zabel RW. Columbia River plume fronts. I. Hydrography, zooplankton distribution, and community composition. Marine Ecology Progress Series. 2005;299: 19–31.

122. Heinemann D. A range finder for pelagic bird censusing. Journal of Wildlife Management. 1981;45: 489–493.

123. Tasker ML, Jones PH, Dixon TIM, Blake BF. Counting seabirds at sea from ships: a review of methods employed and a suggestion for a standardized approach. The Auk. 1984;101: 567–577.

124. Peterson WT, Miller CB. Year-to-year variations in the planktonology of the Oregon upwelling zone. Fishery Bulletin. 1975;73: 642.

125. Peterson WT, Keister JE, Feinberg LR. The effects of the 1997–99 El Niño/La Niña events on hydrography and zooplankton off the central Oregon coast. Progress in oceanography. 2002;54: 381–398.

126. Brodeur RD, Auth TD, Phillips AJ. Major shifts in pelagic micronekton and macrozooplankton community structure in an upwelling ecosystem related to an unprecedented marine heatwave. Frontiers in Marine Science. 2019;6: 212.

127. Miller RR, Santora JA, Auth TD, Sakuma KM, Wells BK, Field JC, et al. Distribution of pelagic thaliaceans, Thetys vagina and Pyrosoma atlanticum, during a period of mass occurrence within the California Current. CalCOFI Rep. 2019;60: 94–108.

128. Northwest Fisheries Science Center. Juvenile Fish Data - Coastwide Cooperative Pre-recruit Survey. 2021. Available: https://www.fisheries.noaa.gov/inport/item/20562

129. Friedman WR, Santora JA, Schroeder ID, Huff DD, Brodeur RD, Field JC, et al. Environmental and geographic relationships among salmon forage assemblages along the continental shelf of the California Current. Marine Ecology Progress Series. 2018;596: 181–198.

130. Keller AA. The 2005 US West Coast bottom trawl survey of groundfish resources off Washington, Oregon, and California: Estimates of distribution, abundance, and length composition. NOAA Technical Memorandum. 2008.

131. Keller AA, Wallace JR, Methot RD. The Northwest Fisheries Science Center's West Coast Groundfish Bottom Trawl Survey: history, design, and description. NOAA Technical Memorandum NMFS-NWFSC-136. 2017.

132. National Marine Fisheries Service WCR. Proposed Revision of the Critical Habitat Designation for Southern Resident Killer Whales. Draft Biological Report. 2019.

Supporting Information

Fig S1. Coastal Upwelling Transport Index (CUTI). The Coastal Upwelling Transport Index (CUTI) is plotted on the y-axis against the day of year (x-axis). Each year (1988-2021) is plotted as an individual line in the blue gradient. The full timeseries (1988-2021) is used to drive the model for comparisons to the vertically generalized production model (VGPM) in Fig 10. The red line in the middle is the average CUTI time series (averaged by day of year across all years), which is used to drive the validation plot in Fig 9.

Fig S2. 100-year model simulation driven by constant upwelling time series. Each living consumer functional group is pictured here as a smoothed individual line. The proportion of abundance relative to starting values are plotted on the y-axis and the daily simulation timestep is plotted on the x-axis (axis in yearly units). The simulation here is driven by a constant value [no seasonal variation; 10% of 1988-2021 Coastal Upwelling Transport Index (CUTI) average] to reduce inter- and intra-annual variation for assessment of equilibrium and model stability. Functional groups in red (both killer whale groups) indicate that populations are increasing by more than 5% in the final 20 years of simulation. All other groups have reached equilibrium (i.e., are within this 5% threshold). No functional groups go extinct over the 100-year simulation. See Fig 9 for a similar simulation driven instead by an average time series that does vary seasonally.

Table S1. Data sources and years included. The table contains information about the sources of both the biomass and diet data for each functional group (rows of table) in the model.

Table S2. Fates of detritus for each functional group. The table contains information about the fates of detritus (eggs, pelagic detritus, fishery offal, benthic detritus, or export from the system) for each functional group (rows of table) in the model. See https://doi.org/10.5281/zenodo.7079777 for a csv version of this table and see Tables 1, S3 – S5 for other ecosystem model parameters.

Table S3. Additional EcoTran parameters. EcoTran parameterization of the model. BA = biomass accumulation and EM = emigration. Detritus fates are listed for feces, senescence and excretion to 2D surface and sub-surface boxes (see Figure 2). Retention scaler indicates the ability of advection to move various functional groups. Advection values of 0 means that groups are physically driven by cross-shelf advection (upwelling and downwelling), while values of 1 means that groups can resist the advection forces. See https://doi.org/10.5281/zenodo.7079777 for a csv version of this table and see Tables 1, S2 – S5 for other ecosystem model parameters.

Table S4. Fishery landings for each functional group. The table contains information about the yearly landings (mt/km^2) of each fishery in the model (columns in table; see Table 2 for descriptions) for each living functional group (rows of table) in the model. See https://doi.org/10.5281/zenodo.7079777 for a csv version of this table and see Tables 1, S2 – S5 for other ecosystem model parameters.

Table S5. Fishery discards for each functional group. The table contains information about the yearly discards (mt/km^2) of each fishery in the model (columns in table; see Table 2 for descriptions) for each living functional group (rows of table) in the model. See https://doi.org/10.5281/zenodo.7079777 for a csv version of this table and see Tables 1, S2 – S5 for other ecosystem model parameters.

Table S6. Stability in 100-year simulations. The table contains percent change in the last 20 years of a 100-year simulation with an average CUTI upwelling timeseries (see Figure 9) for each functional group (rows of table) in the model.

Appendix

Biomass sources

Coastal Pelagic Species

The SWFSC coastal pelagic species (CPS) acoustic-trawl survey is a north-to-south coastwide survey that pairs backscatter data from a multi-frequency echosounder and nighttime trawls to provide biomass estimates for Pacific sardine, Pacific herring, Pacific chub mackerel, Pacific jack mackerel, and northern anchovy [53,54]. The CPS survey sampling domain fully covers the spatial domain of EcoTran (in both latitude and bathymetry). We used data from 2015-2019 to parameterize sardine, anchovy, herring, jack mackerel, and chub mackerel.

Pacific Hake Ecosystem Acoustic Trawl Survey

The NWFSC conducts a joint US-Canada coastwide acoustic-trawl survey for Pacific hake (hereafter hake survey) during July and August in odd years (e.g., 2015, 2017). The hake survey sampling domain fully covers the spatial domain of EcoTran (in both latitude and bathymetry). The survey pairs fisheries acoustics data from multi-frequency echosounders with midwater trawls to estimate Pacific hake biomass for stock assessment [59,60], and uses frequency differencing and an inversion model to estimate euphausiid biomass for ecosystem monitoring and research [115,116]. We used data from 2015, 2017, and 2019 to parameterize krill and hake biomasses.

Juvenile Salmon and Ocean Ecosystem Survey (JSOES)

The Juvenile Salmon and Ocean Ecosystem Survey is a long-term (1998-present) survey, which provided data on the pelagic community composition for salmonids, zooplankton, and seabirds from daytime surveys of the shelf off Oregon and Washington (between 44.25°N and 48.23°N) each year during May, June, and/or September [117,118]. JSOES does not extend to the southern-most subregions of the EcoTran domain. Yet, it consistently samples within all three of our cross-shelf bathymetric zones. Juvenile and adult salmon and jellies were collected during daylight hours using a Nordic 264 pelagic rope trawl with a mouth opening of 30 m wide and 20 m height with a 0.8 cm cod-end liner. The net was typically towed for 30 minutes at the surface with a ship speed of ~6 km h^{-1} (3.2 knots).

Zooplankton were sampled via bongo tows and vertical nets [119,120]. A 0.60 m diameter Bongo net (equipped with two black 335 µm mesh nets), is used to conduct double oblique plankton tows. The bongo net is fished such that a maximum depth of 20 to 30 m is reached. For the vertical net samples, a 0.5 m ring net (202 µm mesh) is used to collect a vertical plankton tow from 100 m, or 5 m from the bottom in shallower locations. For both zooplankton nets, flow meters are used to measure the volume of water filtered through the nets so that the prey densities can be calculated.

Seabird abundance and distributions were estimated from visual detections of birds within a bow-to-beam, 300 m wide arc (strip-transect method) [121,122]. To avoid having trawl activity affect bird distributions, surveys began at dawn ~ 33 km offshore of the inshore-most sampling

station, prior to any fishing operations. A trained observer used binoculars (8 x 42 mm) to detect, count, and identify birds within the survey strip. Each bird detection was recorded with a date, time, and position stamp into the custom "SeeBird" data acquisition software (NMFS Southwest Fisheries Science Center, La Jolla, CA).

Newport Hydrographic Line

The Newport Hydrographic Line is a long-term, single cross-shelf transect survey off the central Oregon coast [123,124], which occurs year-round at bi-weekly to monthly intervals. Observations from the survey allowed us to parameterize small invertebrate larvae and invertebrate (copepod and euphausiid) egg biomass. Mesozooplankton and egg densities are from two stations located on the inner shelf and outer shelf in 60 m and 300 m of water respectively. Smaller zooplankton were collected with a 0.5 m net fitted with 200 um mesh and hauled vertically from 100 m (or 5 m off the seafloor in depths shallower than 100 m). The Newport Hydrographic Line also provided data allowing us to partition the biomass of phytoplankton (from satellite imagery, described in main text) into large and small phytoplankton groups (see Table 2) and euphausiids (from the hake survey, described above) into the two dominant euphausiid species in the NCC, *Thysanoessa spinifera* and *Euphausia pacifica.* Biomass of the two krill species, *T. spinifera* and *E. pacifica*, were collected at night with a 0.6 m net towed obliquely over the upper 30 m of the water column at three stations located on the inner shelf and outer shelf in 60 m, 80 m, and 300 m of water.

Pre-recruit survey

The Pre-recruit survey is a midwater trawl survey that occurs annually (2011, 2013-2019, 2022) around May-July along transects located along the Washington, Oregon, and Northern California coasts . Stations are arrayed along cross-shelf transects set at every half degree of latitude both on and off the shelf. Stations are sampled cross-shelf past the EcoTran domain defined here, thus the Pre-recruit survey fully covers the spatial domain of EcoTran. A modified-Cobb midwater trawl with a 26 m headrope and a 9.5 mm cod-end liner is used to sample epipelagic micronekton at night with the headrope at around 30 m depth. This survey primarily samples micronektonic squid, shrimp, krill, larger gelatinous zooplankton, and mesopelagic and juvenile fish [129].

West Coast Groundfish Bottom Trawl Survey

The NWFSC West Coast Groundfish Bottom Trawl Survey (hereafter groundfish survey) occurs annually from May-October, and uses a random stratified design to sample the entire west coast of the United States via a bottom trawl from 55-1280 m depths [130,131]. Thus the groundfish survey fully covers the spatial domain of EcoTran. Data from 2003-2019 are available via the `nwfscSurvey` R package [62]. We used data from 2014-2019 to parameterize many groups of groundfish and crabs (see Table S1).

Diet sources

California Current Trophic Database

The California Current Trophic Database (https://oceanview.pfeg.noaa.gov/cctd/) was conceived and developed at the National Marine Fisheries Service (NMFS) Southwest Fisheries Science

Center (SWFSC) in collaboration with trophic data contributors. The trophic database was compiled from twenty-four data sets, including stomach or scat contents, which were contributed from collaborators at the NOAA NMFS [SWFSC; NWFSC; and AFSC (Alaska Fisheries Science Center)], and academic institutions (University of California, Santa Cruz; Oregon State University; and Moss Landing Marine Laboratories). Once acquired, data were reviewed, standardized with communication and input from contributors, and synthesized. In total, diet composition data were obtained from 105,694 individual predators among 143 taxa collected throughout the California Current Large Marine Ecosystem from 1967–2019. These taxa consist of squids (n=5), elasmobranchs (n=13), bony fishes (n=118), and marine mammals (n=7).

The trophic database was created using the Structured Query Language (SQL) and consists of eight data tables. Hierarchical (parent-child) tables include Data Sources, Collection Information, Predator Information, Prey Composition, and Prey Size. The trophic database contains two taxonomic tables, one for predators (n=143) and one for prey (n=1659), that are linked to the Predator Information and Prey Composition tables. The World Register of Marine Species (WoRMS; https://www.marinespecies.org/) was primarily used for taxonomic reference, and scientific names from each data set were updated accordingly. Additional taxonomic resources (e.g., recent primary literature, California Academy of Fishes Fish Catalog) were incorporated when WoRMS designations seemed dated or unsubstantiated. A single flat file that was created from the five hierarchical SQL tables is provided to the public via SWFSC's ERDDAP site, along with Glossary, Predator Taxonomy, and Prey Taxonomy tables. Predator diets were processed as described in the main text.

Juvenile salmon diets

Juvenile salmon stomach content data were collected from the JSOES survey (see survey description above). Prey items were removed from stomachs and identified to the lowest possible taxonomic level, counted, and weighed to the nearest 1 mg. Salmon with empty stomachs were removed from the analysis since these data are uninformative for parameterizing diet contributions. Similarly, since we broke out juvenile Chinook salmon into multiple functional groups (Table 2; see "Salmonids" subheading in main text) based on genetic stock information, those observations without associated genetic stock information were removed as they are also unable to inform the diets of our various salmon functional groups. All unidentified prey material and non-living material (i.e., plastic) were also removed from the diets. Then we calculated the relative contribution of each species or taxonomic group as prey (allocated to and aggregated by our functional groups in Table 2) to each of the juvenile salmonid functional groups by summing the weights of prey groups and dividing by the total weight of prey consumed for that juvenile salmonid group (see supplementary code and diet matrix for more information).

Tables

Table 1: NCC EcoTran parameters.

Ecopath parameterization of the model. TL = estimated trophic level, Biomass = estimated average biomass density in ecosystem (mt/km^2), P/B = weight-specific production rate, C/B = weight-specific consumption rate, EE = ecotrophic efficiency. EE values are estimated by the Ecopath master equation (see equation 1 in main text), except those in which biomass needed to be estimated (EE in bold). See https://doi.org/10.5281/zenodo.7079777 for a csv version of this table and see Tables S2 – S5 for other ecosystem model parameters.

#	Functional group	TL	Biomass	P/B	C/B	EE
1	Large phytoplankton	1.00	45.753	215.00	–	0.980
2	Small phytoplankton	1.00	6.230	215.00	–	0.945
3	Micro-zooplankton	2.00	16.219	150.00	428.57	**0.900**
4	Large copepods	2.25	6.552	15.00	60.00	0.744
5	Small copepods	2.35	26.443	37.00	148.00	0.419
6	Small invertebrate larvae	2.35	4.813	37.00	148.00	0.573
7	Pteropods	2.53	0.272	15.00	50.00	0.759
8	Pelagic amphipods	2.65	0.662	14.00	56.00	0.734
9	Pelagic shrimp	3.27	18.939	3.00	12.00	0.885
10	Other macro-zooplankton	2.88	6.309	10.00	40.00	0.726
11	Small jellyfish (net-feeders)	2.40	1.671	45.00	150.00	0.021
12	Small jellyfish (carnivores)	3.48	0.054	20.00	66.67	0.023
13	Large jellyfish	3.08	0.101	15.00	60.00	0.079
14	Pyrosomes	2.08	15.976	45.00	150.00	0.001
15	*E. Pacifica*	2.30	32.294	6.00	24.00	0.932
16	*T. Spinifera*	2.30	10.234	7.00	28.00	0.799
17	Small cephalopod aggregate	3.63	2.640	3.00	12.00	**0.850**
18	Cephalopod humboldt	4.36	0.005	2.75	11.00	0.969
19	Smelt aggregate	3.65	7.383	1.80	7.20	0.821
20	Shad	3.34	2.081	1.13	4.53	**0.900**
21	Sardine	3.11	1.841	1.13	4.53	0.966

#	Functional group	TL	Biomass	P/B	C/B	EE
22	Herring	3.17	4.099	1.80	7.20	0.943
23	Anchovy	3.19	3.038	1.80	7.20	0.860
24	Saury	3.75	0.130	1.13	4.53	0.775
25	Coho yearling	4.28	0.222	1.80	7.20	0.933
26	Chinook yearling spring-run	4.20	0.110	1.13	4.53	0.881
27	Chinook yearling fall-run	4.24	0.080	1.13	4.53	0.834
28	Chinook subyearling fall-run early	3.94	0.015	1.80	7.20	0.841
29	Chinook subyearling fall-run late	4.19	0.094	1.80	7.20	0.820
30	Other Chinook yearling	4.31	0.014	1.13	4.53	0.956
31	Other Chinook subyearling	4.07	0.057	1.80	7.20	0.961
32	Other juvenile salmon	3.46	0.028	1.80	7.20	0.855
33	Mesopelagic fish aggregate	3.36	1.245	1.75	7.00	**0.850**
34	Planktivorous rockfish	3.76	6.420	0.13	1.25	0.952
35	Coho	4.17	0.230	1.80	10.59	0.739
36	Chinook	4.07	0.112	0.75	4.41	0.892
37	Other salmon aggregate	3.98	0.019	1.90	11.18	0.756
38	Shark aggregate	4.73	0.017	0.20	3.33	0.788
39	Jack mackerel	3.64	21.395	0.23	2.30	0.103
40	Pacific mackerel	3.49	0.857	0.76	7.60	0.848
41	Piscivorous rockfish	3.88	3.072	0.17	1.72	0.980
42	Dogfish aggregate	4.21	3.475	0.20	2.50	0.272
43	Hake	3.65	18.500	0.35	3.54	0.987
44	Tuna aggregate	4.29	0.200	0.30	3.00	0.893
45	Sablefish	4.16	1.787	0.23	2.30	0.952
46	Hexagrammidae (lingcod greenling)	4.43	0.722	0.30	3.00	0.905
47	Flatfish (water-column feeders)	4.29	3.797	0.28	1.38	0.817
48	Skates & rays	3.71	2.769	0.23	2.30	0.266

#	Functional group	TL	Biomass	P/B	C/B	EE
49	Misc. Small benthic fishes	3.33	8.900	0.40	4.00	**0.900**
50	Benthivorous rockfish	3.67	7.987	0.07	0.70	0.811
51	Gadidae (cod haddock pollock)	3.48	0.120	0.35	3.50	0.838
52	Flatfish (benthic feeders)	3.16	11.878	0.30	3.00	0.684
53	Flatfish (small)	3.45	7.968	0.38	1.90	0.919
54	Grenadier	3.62	1.206	0.20	1.00	0.066
55	Juvenile rockfish	3.51	1.202	2.70	10.80	0.930
56	Juvenile fish (other)	3.26	5.991	2.70	10.80	0.735
57	Juvenile fish (chondrichthyes)	3.44	0.535	2.70	10.80	**0.850**
58	Infauna	2.00	80.000	4.50	18.00	0.973
59	*Pandalus spp.*	2.91	14.257	3.00	12.00	0.903
60	Other epibenthic shrimp (Caridea)	2.81	12.950	4.20	16.80	**0.850**
61	Mysids	2.83	2.637	22.00	110.00	**0.850**
62	Echinoderms	2.07	21.361	1.21	6.05	**0.850**
63	Benthic amphipods isopods and cumaceans	2.05	7.158	21.50	107.50	**0.850**
64	Bivalves	2.03	64.450	1.30	6.50	**0.850**
65	Misc. Epifauna (suspension feeders)	2.14	3.828	7.40	37.00	**0.850**
66	Dungeness crab	3.27	5.109	1.50	6.00	0.952
67	Tanner crab	2.99	0.869	1.00	4.00	0.939
68	Misc. Epifauna (carnivorous)	2.67	31.550	3.00	15.00	**0.850**
69	Sooty shearwaters	4.31	0.017	0.10	73.00	0.014
70	Common murre	4.37	0.015	0.17	72.00	0.210
71	Gulls & terns	3.79	0.001	0.17	73.00	0.774
72	Alcids	3.90	0.001	0.17	110.00	0.084
73	Large pelagic seabirds	4.08	0.001	0.07	75.00	0.128
74	Other pelagic seabirds	4.29	0.001	0.10	73.00	0.046
75	Coastal seabirds (divers)	4.29	0.001	0.16	73.00	0.218

#	Functional group	TL	Biomass	P/B	C/B	EE
76	Storm-petrels	3.86	0.0001	0.12	144.00	0.072
77	Gray whales	3.72	0.146	0.06	8.90	0.002
78	Baleen whales	3.69	0.572	0.04	7.60	0.002
79	Small pinnipeds	4.55	0.024	0.08	8.30	0.034
80	Sea lions	4.64	0.049	0.07	24.00	0.279
81	Northern elephant seals	4.49	0.062	0.07	24.00	0.219
82	Small toothed whales	4.44	0.072	0.10	25.80	0.112
83	Large toothed whales	4.57	0.067	0.05	6.61	0.003
84	Other killer whales	4.94	0.0004	0.03	11.16	0.000
85	Southern resident killer whales	5.13	0.005	0.03	11.16	0.000
86	Invertebrate eggs	1.00	0.00002	0.00	0.00	0.225
87	Fish eggs	1.00	1.906	0.00	0.00	0.421
88	Pelagic detritus	1.00	10.000	0.00	0.00	0.525
89	Fishery offal	1.00	5.000	0.00	0.00	0.684
90	Benthic detritus	1.00	10.000	0.00	0.00	0.885
91	Dredge	3.04	--	--	--	--
92	Hook & line	5.16	--	--	--	--
93	Other gear	4.57	--	--	--	--
94	Net	4.34	--	--	--	--
95	Pot & trap	4.53	--	--	--	--
96	Trolling	5.23	--	--	--	--
97	Trawl (non-shrimp)	4.67	--	--	--	--
98	Shrimp trawls	3.97	--	--	--	--
99	Recreational fishery	5.07	--	--	--	--

Table 2: Functional group definitions.

Functional group names and description of composition. See Table S1 for a description of the data sources. See supplemental data for csv version of table.

Functional group	Group composition
Large phytoplankton	>10 um (large chain and centric diatoms)
Small phytoplankton	≤ 10 um (cyanobacteria, dinoflagellates, small diatoms)
Micro-zooplankton	Ciliates, flagellate grazers
Large copepods	Copepods ≥ 0.025 mg C
Small copepods	Copepods < 0.025 mg C
Small invertebrate larvae	Copepods (nauplii), small crustacean larvae (zoea, cypids), euphausiid (larvae), mollusk larvae (veligers), echinoderm larvae (pluteus), other invert larvae
Pteropods	Order: Pteropoda
Pelagic amphipods	Hyperiidae, Gammaridae
Pelagic shrimp	Sergestidae, Penaeidae
Other macro-zooplankton	Chaetognaths, large crustacean larvae (megalopae), ichthyoplankton, other macro-zooplankton (pelagic polychaetes, heteropods, ostracods, cladocerans)
Small jellyfish (net-feeders)	Urochordates (larvaceans, salps)
Small jellyfish (carnivores)	Ctenophores, misc. Small medusae
Large jellyfish	Sea nettle (*Chrysaora fuscescens*), moon jelly (*Aurelia labiata*), egg yolk jelly (*Phacellophora camtschatica*), water jelly (*Aequorea spp.*), lion's mane jelly (*Cyanea capillata*)
Pyrosomes	*Pyrosoma atlanticum*
E. pacifica	*Euphausia pacifica* (adult & juveniles)
T. spinifera	*Thysanoessa spinifera* (adult & juveniles)
Small cephalopods	Market squid (*Doryteuthis opalescens*)
Humboldt squid	Humboldt squid (*Dosidicus gigas*)
Smelt aggregate	Pacific sand lance (*Ammodytes hexapterus*), jacksmelt/silversides *(Atherinopsis californiensis)*, eulachon *(Thaleichthys pacificus)*, night smelt *(Spirinchus starksi)*, longfin smelt *(Spirinchus thaleichthys)*, surf smelt *(Hypomesus pretiosus)*, whitebait smelt *(Allosmerus elongates)*, popeye blacksmelt *(Bathylagus ochotensis)*
Shad	American shad *(Alosa sapidissima)*
Sardine	Pacific sardine *(Sardinops sagax)*
Herring	Pacific herring *(Clupea pallasii)*
Anchovy	Northern anchovy *(Engraulis mordax)*
Saury	Pacific saury *(Cololabis saira)*
Juvenile coho	Juvenile Coho salmon (*Oncorhynchus kisutch*) yearling
Juvenile Chinook Y spring	Juvenile Chinook salmon *(Oncorhynchus tshawytscha)* spring-run yearlings (Columbia River + Washington coast stocks)
Juvenile Chinook Y fall	Juvenile Chinook salmon *(O. tshawytscha)* fall-run yearlings (Columbia River + Washington coast stocks)
Juvenile Chinook SY fall early	Juvenile Chinook salmon *(O. tshawytscha)* fall-run subyearlings; early ocean migrants (May and June JSOES surveys; Columbia River + Washington coast stocks)
Juvenile Chinook SY fall late	Juvenile Chinook salmon *(O. tshawytscha)* fall-run subyearlings; late ocean migrants (September JSOES surveys; Columbia River + Washington coast stocks)
Other juv. Chinook Y	All other juvenile Chinook salmon *(O. tshawytscha)* yearlings
Other juv. Chinook SY	All other juvenile Chinook salmon *(O. tshawytscha)* subyearlings

Other juvenile salmon	All juvenile salmon not described above: pink *(Oncorhynchus gorbuscha)*, chum *(O. keta)*, sockeye *(O. nerka)*, steelhead *(O. mykiss)*
Mesopelagic fish aggregate	Myctophidae, Bathylagidae, Lophotidae (Crestfishes), Ophidiidae (cusk eel), Paralepididae (barracudina), Stomiidae (dragonfish), Trachipteridae (ribbonfishes), Nemichthyidae (snipe eels)
Planktivorous rockfish	Aurora *(Sebastes aurora)*, bank *(S. Rufus)*, blue *(S. Mystinus)*, darkblotched *(S. Crameri)*, greenstriped *(S. Elongates)*, harlequin *(S. Variegatus)*, Pacific Ocean perch *(S. Alutus)*, Puget Sound *(S. Emphaeus)*, pygmy *(S. Wilsoni)*, redstripe *(S. Proriger)*, rosy *(S. Rosaceus)*, sharpchin *(S. Zacentrus)*, shortbelly *(S. Jordani)*, splitnose *(S. Diploproa)*, stripetail *(S. Saxicola)*, widow *(S. Entomelas)*, yellowmouth *(S. Reedi)*
Coho	Adults: *(Oncorhynchus kisutch)*
Chinook	Adults: *(Oncorhynchus tshawytscha)*
Other salmon aggregate	Adults: pink *(Oncorhynchus gorbuscha)*, chum *(O. keta)*, sockeye *(O. nerka)*, steelhead *(O. mykiss)*, cutthroat trout *(O. mykiss)*
Shark aggregate	Tope (a.k.a soupfin; *Galeorhinus galeus)*, blue *(Prionace glauca)*, thresher *(Alopias vulpinus)*, salmon *(Lamna ditropis)*, shortfin mako *(Isurus oxyrinchus)*
Jack mackerel	Jack mackerel *(Trachurus symmetricus)*
Pacific mackerel	Pacific chub mackerel *(Scomber japonicus)*
Piscivorous rockfish	Black *(Sebastes melanops)*, blackgill *(S. Melanostomus)*, bocaccio *(S. Paucispinis)*, canary *(S. Pinniger)*, chilipepper *(S. Goodie)*, yelloweye *(S. Ruberrimus)*, yellowtail *(S. Flavidus)*
Dogfish aggregate	Spiny dogfish *(Squalus acanthias)*, brown catshark *(Apristurus brunneus)*, filetail catshark *(Parmaturus xaniurus)*, Pacific sleeper shark *(Somniosus pacificus)*
Hake	Pacific hake *(Merluccius productus)*
Tuna aggregate	Albacore *(Thunnus alalunga)*, Pacific barracuda *(Sphyraena argentea)*, bigeye tuna *(T. obesus)*, bluefin tuna *(T. thynnus)*, Bramidae (pomfret), Carangidae (jacks, pompanos), yellowtail tuna *(T. albacares)*, Pacific bonito *(Sarda chiliensis)*
Sablefish	Sablefish *(Anoplopoma fimbria)*
Hexagrammidae (lingcod greenling)	Lingcod *(Ophiodon elongates)*, greenling *(Hexagrammos decagrammus)*
Flatfish (water-column feeders)	Pacific halibut *(Hippoglossus stenolepis)*, arrowtooth flounder *(Atheresthes stomias)*, petrale sole *(Eopsetta jordani)*, California halibut *(Paralichthys californicus)*
Skates & rays	Bat ray *(Myliobatis californica)*, big skate *(Raja binoculata)*, black skate *(Bathyraja trachura)*, Pacific electric ray *(Torpedo californica)*, longnose skate *(Raja rhina)*, Pacific angelshark *(Squatina californica)*, spotted ratfish *(Hydrolagus colliei)*
Misc. Small benthic fishes	Agonidae (poachers), Bathymasteridae (ronquils), Batrachoididae (Toadfishes), Blenniidae (blennies), Cottidae (sculpins), Cyclopteridae (lumpfish), Embiotocidae (surfperch), Gasterosteidae (sticklebacks), Gobiidae (gobies), hagfish, Kyphosidae (sea chubs), lamprey eels, Liparidae (snailfish), Moronidae (striped bass), Pholidae (gunnels), prowfish, Sciaenidae (drums, croakers), Stichaeidae (prickleback), Syngnathidae (pipefishes), Triglidae (Searobins), Zoarcidae (eelpout)
Benthivorous rockfish	Cabezon *(Scorpaenichthys marmoratus)*, longspine thornyhead *(Sebastolobus altivelis)*, shortspine thornyhead *(Sebastolobus alascanus)*, copper *(Sebastes caurinus)*, quillback *(S. maliger)*, redbanded *(S. babcocki)*, rosethorn *(S. helvomaculatus)*, rougheye *(S. aleutianus)*, shortraker *(S. borealis)*, silvergray *(S. brevispinis)*, tiger *(S. nigrocinctus)*

Gadidae (cod haddock pollock)	Pacific cod *(Gadus macrocephalus)*, walleye pollock *(Theragra chalcogramma)*, Pacific tomcod *(Microgadus proximus)*
Flatfish (benthic feeders)	English sole *(Parophrys vetulus)*, Dover sole *(Microstomus pacificus)*, rex sole *(Glyptocephalus zachirus)*
Flatfish (small)	Butter sole *(Isopsetta isolepis)*, curlfin sole *(Pleuronichthys decurrens)*, deepsea sole *(Embassichthys bathybius)*, flathead sole *(Hippoglossoides elassodon)*, rock sole *(Lepidopsetta bilineata)*, sand sole *(Trulla capensis)*, sanddabs *(Citharichthys spp.)*, slender sole *(Lyopsetta exilis)*, starry flounder *(Platichthys stellatus)*, Pleuronectidae (turbot)
Grenadier	Giant grenadier *(Albatrossia pectoralis)*, Pacific grenadier *(Coryphaenoides acrolepis)*
Juvenile rockfish	Thornyheads, Greenlings, Painted greenling, Lingcod, Sculpins, Irish lords, Red Irish lord, Brown Irish lord, Cabezon, All rockfish (Sebastidae)
Juvenile fish (other)	American shad, Pacific herring, Pacific sardine, Northern anchovy, Pacific hake, Pacific tomcod, Sablefish, Wolf eel, Eel leptocephalus, Jack mackerel, Pacific chub mackerel, Pacific sanddab, Speckled sanddab, Righteye flounders, Arrowtooth flounder, Deepsea sole, Rex sole, Flathead sole, Butter sole, Rock sole, Slender sole, Dover sole, English sole, Soles/Turbits/Flounders, Curlfin turbot, Sand sole
Juvenile fish (chondrichthys)	Juvenile sharks, skates, and rays
Infauna	Misc. Benthic organisms living in ocean floor substrate
Pandalus spp.	Pink shrimp *(Pandalus jordani)*
Other epibenthic shrimp (caridea)	*Crangon spp.*, *Callianassa spp.*, *Pasiphaea pacifica*
Mysids	Mysids & cumaceans
Echinoderms	Red sea urchin *(Mesocentrotus franciscanus)*, purple sea urchin *(Strongylocentrotus purpuratus)*, misc. brittle stars, misc. Sea cucumbers, (NOTE: does not include starfish)
Benthic amphipods isopods and cumaceans	Benthic amphipods, isopods, cumaceans
Bivalves	Basket cockle *(Clinocardium nuttallii)*, butter clam *(Saxidomus gigantean)*, California mussel *(Mytilus californianus)*, gaper clam *(Tresus capax)*, Manila clam *(Venerupis philippinarum)*, native littleneck clam *(Leukoma staminea)*, rock scallop *(Crassadoma gigantean)*, Weathervane scallops *(Patinopecten caurinus)*, Pacific oyster *(Crassostrea gigas)*, razor clam *(Siliqua patula)*, soft-shelled clam *(Mya arenaria)*, purple varnish clam *(Nuttallia obscurata)*, rough paddock *(Zirfaea pilsbryi)*, flat tipped piddock *(Penitella penita)*
Misc. Epifauna (suspension feeders)	Barnacles, bryozoans, sea anemones
Dungeness crab	Dungeness crab *(Cancer magister)*
Tanner crab	Bairds tanner crab *(Chionoecetes bairdi)*, grooved tanner crab *(Chionoecetes tanneri)*, triangle tanner crab *(Chionoecetes angulatus)*
Misc. Epifauna (carnivorous)	Misc. Small crabs, misc. Gastropods, starfishes
Sooty shearwaters	Sooty shearwaters *(Puffinus griseus)*
Common murre	Common murre *(Uria aalge)*
Gulls & terns	California gull *(Larus californicus)*, glaucous-winged gull *(L. Glaucescens)*, Heermann's gull *(L. heermanni)*, herring gull *(L. Argentatus)*, ring-billed gull *(L. Delawarensis)*, Sabine's gull *(Xema sabini)*, western gull *(L. Occidentalis)*, hybrid gulls, arctic tern *(Sterna paradisaea)*, Caspian tern *(S. caspia)*, common tern *(S. Hirundo)*

Alcids	Cassin's auklet *(Ptychoramphus aleuticus)*, rhinoceros auklet *(Cerorhinca monocerata)*, pigeon guillemot *(Cepphus columba)*, marbled murrelet *(Brachyramphus marmoratus)*, ancient murrelet *(Synthliboramphus antiquus)*, tufted puffin *(Fratercula cirrhata)*, horned puffin *(F. Corniculata)*
Large pelagic seabirds	Black-footed albatross *(Phoebastria nigripes)*, Laysan albatross *(Phoebastria immutabilis)*, parasitic jaeger *(Stercorarius parasiticus)*, northern fulmar *(Fulmarus glacialis)*, skuas, petrels
Other pelagic seabirds	Buller's shearwater *(Puffinus bulleri)*, flesh-footed shearwater *(Puffinus carneipes)*, pink-footed shearwater *(Puffinus creatopus)*, red-necked Phalarope *(Phalaropus lobatus)*, other murres
Coastal seabirds (divers)	Brown pelican *(Pelecanus occidentalis)*, white pelican *(Pelecanus erythrorhynchos)*, Brandt's cormorant *(Phalacrocorax penicillatus)*, double-crested cormorant *(Phalacrocorax auritus)*, pelagic cormorant *(Phalacrocorax pelagicus)*, western grebe *(Aechmophorus occidentalis)*, Clark's grebe *(Aechmophorus clarkii)*
Storm-petrels	Fork-tailed storm petrel *(Oceanodroma furcata)*, Leach's storm-petrel *(Oceanodroma leucorhoa)*
Gray whales	Gray whales *(Eschrichtius robustus)*
Baleen whales	Minke whale *(Balaenoptera acutorostrata)*, humpback whale *(Megaptera novaeangliae)*, sei whale *(Balaenoptera borealis)*, fin whale *(Balaenoptera physalus)*, blue whale *(Balaenoptera musculus)*
Small pinnipeds	Harbor seal *(Phoca vitulina richardsi)*, Northern fur seal *(Callorhinus ursinus)*
Sea lions	California sea lion *(Zalophus californicus)*, Steller's sea lion *(Eumetopias jubatus)*
N. elephant seals	Northern elephant seal *(Mirounga angustirostris)*
Small toothed whales	Harbor porpoise *(Phocoena phocoena)*, Dall's porpoise *(Phocoenoides dalli)*, Pacific white-sided dolphin *(Lagenorhynchus obliquidens)*, Risso's dolphin *(Grampus griseus)*, northern right whale dolphin *(Lissodelphis borealis)*
Large toothed whales	Sperm whale *(Physeter catadon)*, pilot whale *(Globicephala macrorhynchus)*, Baird's beaked whale *(Berardius bairdii)*, mesoplodon beaked whale *(Mesoplodon spp.)*, Cuvier's beaked whale *(Ziphius cavirostris)*
Other killer whales	Killer whales *(Orcinus orca)*
SRKW	Southern resident killer whales *(Orcinus orca)*
Invertebrate eggs	Invertebrate eggs
Fish eggs	Fish eggs
Pelagic detritus	Pelagic detritus
Fishery offal	Fishery offal
Benthic detritus	Benthic detritus
Dredge	Dredge fishery
Hook & line	Hook and line fishery
Other gear	Other gear / miscellaneous
Net	Non-trawl nets (e.g., Gill-net, etc.)
Pot & trap	Pots and traps
Trolling	Trolling fishery
Trawl (non-shrimp)	Non-shrimp trawls
Shrimp trawls	Shrimp trawls
Recreational fishery	Recreational fishing

Figures

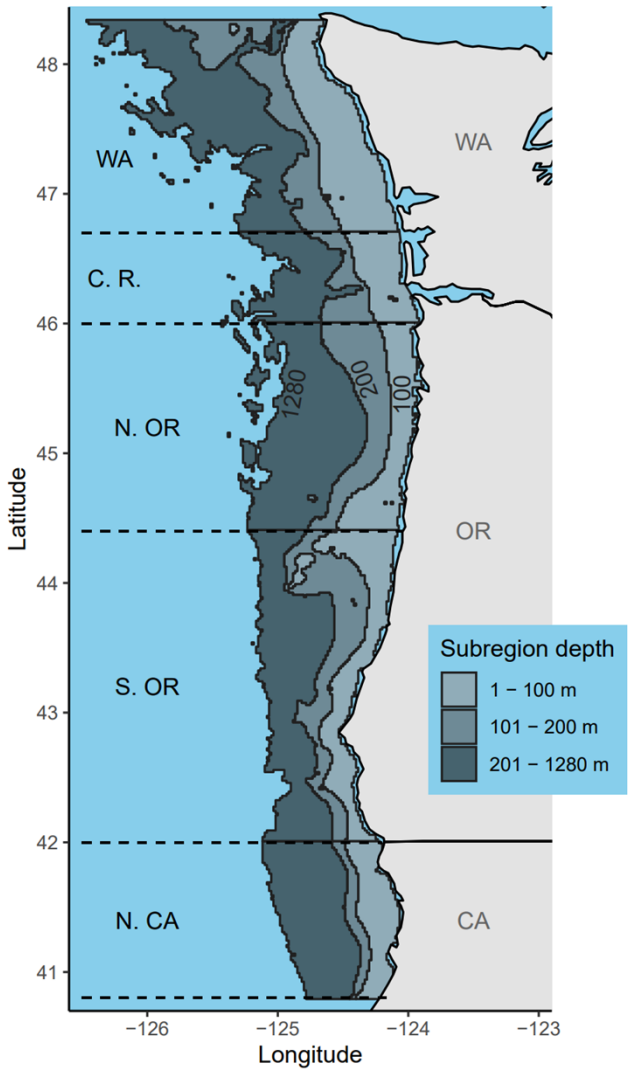

Fig 1: Map of Northern California Current

Extent of end-to-end ecosystem model in the Northern California Current marine ecosystem. Shaded gray bins indicate the 15 ecosystem model subregions. The model domain is broken down into three bathymetric bins (inner shelf: 1 – 100 m; mid shelf: 101 – 200 m; and outer shelf: 201 – 1280 m) and five latitudinal bins (northern California: 40.8 – 42 °N; southern Oregon: 42 – 44.4 °N; northern Oregon: 44.4 – 46 °N; Columbia River zone: 46 – 46.7 °N; and Washington coast: 46.7 – 48.34 °N).

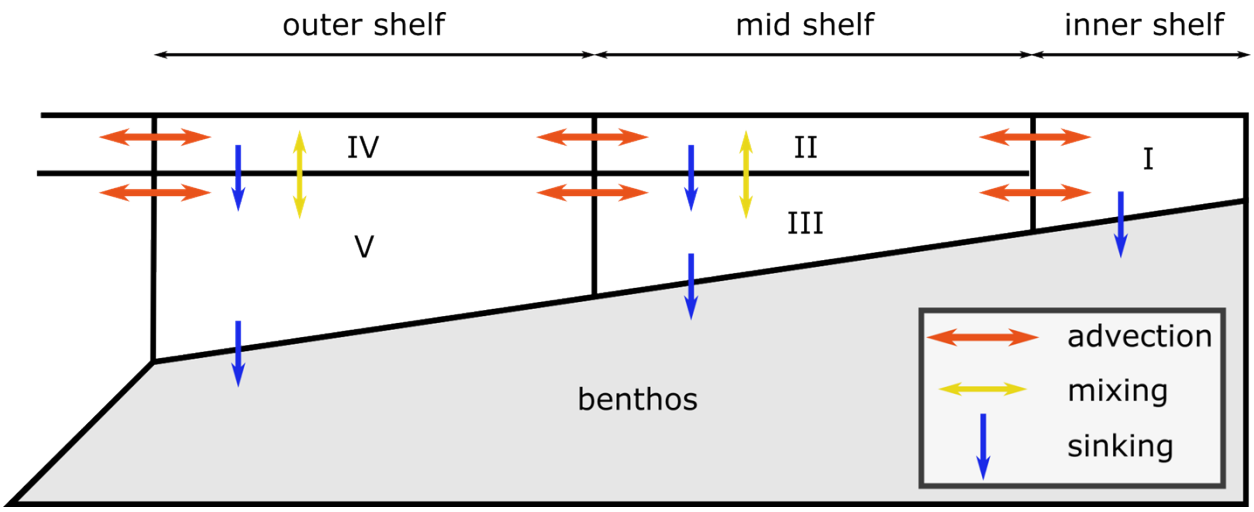

Fig 2: Cross-shelf physical model

The EcoTran ecosystem model allows direct linking of physical oceanographic forcings to the food web model, which drives primary production and the transport of plankton, detritus, and nutrients across model domain boundaries. The currency of a time-dynamic EcoTran model (see Fig 9 and 10 for examples) is nitrogen input to the system as nitrate and ammonium at the base of the food web via upwelling and detritus remineralization by bacteria. The ecosystem model is driven by nutrient flux that is important for bottom-up food web processes using the coastal upwelling transport index (CUTI) [41]. The CUTI time series (in daily time steps) drives advection (red arrows) of nutrients across the shelf. Primary production is supported by nutrient uptake and, in turn, supports grazing and predation by higher trophic level groups and catch by fishing fleets.

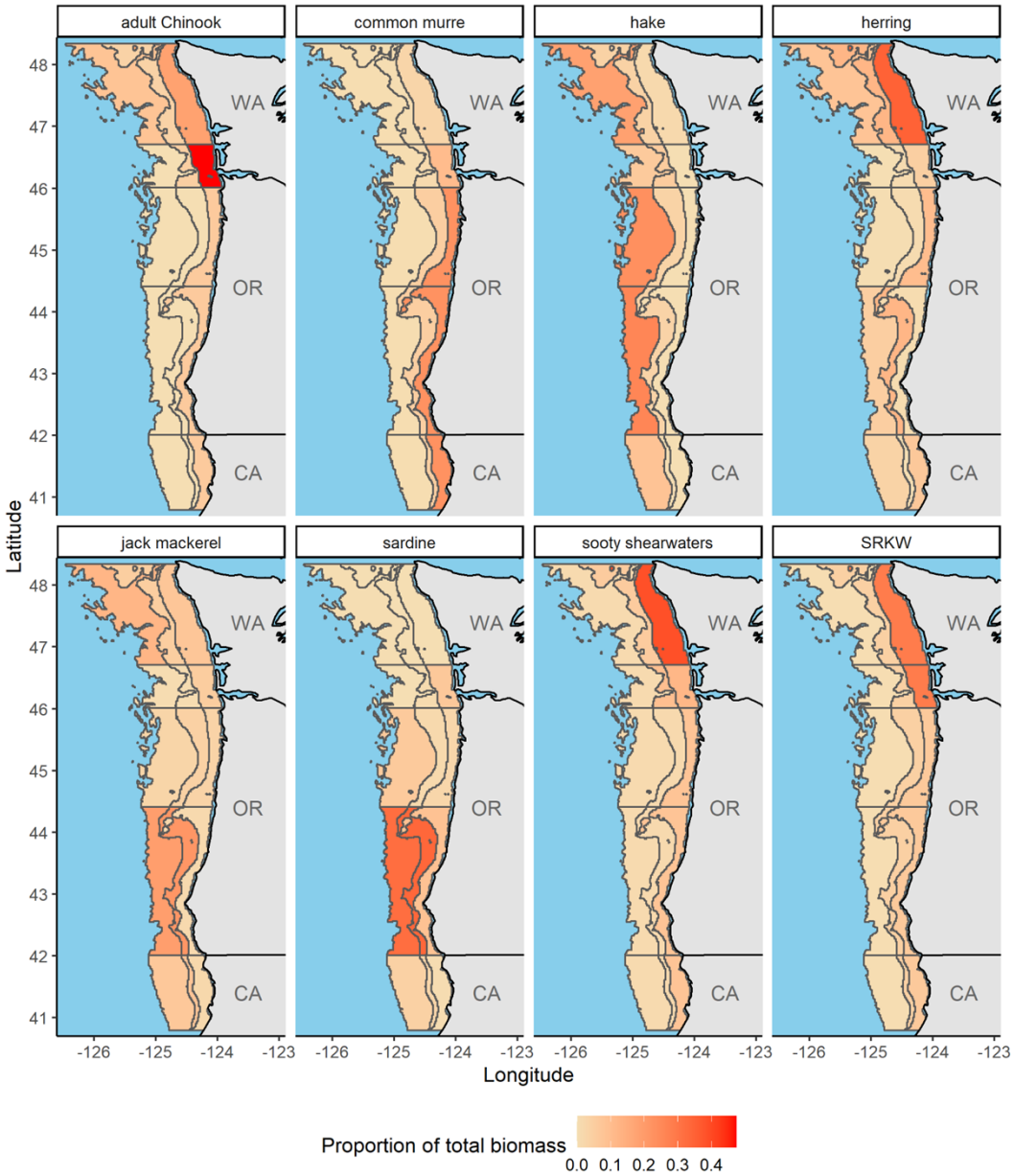

Fig 3: Subregional heatmaps of functional group spatial distributions

Each functional group was broken out into the 15 subregions via survey data, fisheries landings data, or species distribution models (see Methods), or distributional assumptions when there was a lack of available information. The color of each subregional cell is a gradient denoting the proportion of biomass (for each functional group) that is within each subregional cell (with red being the highest and pale yellow being the lowest proportions, respectively). The proportion of

biomass in each subregion sums to 1 across all subregions. See “SubRegions/” in supplemental data and code to reproduce this plot, and for plots of all functional groups). Adult Chinook, common murre, and sooty shearwater distributions are based off of the juvenile salmon and ocean ecosystem survey (JSOES); hake distributions are from the hake acoustic trawl survey; herring, jack mackerel, and sardine distributions are from the coastal pelagic species (CPS) acoustic trawl survey; and Southern resident killer whale (SRKW) distributions are based off of movement data from satellite-tagged Southern resident killer whales [132].

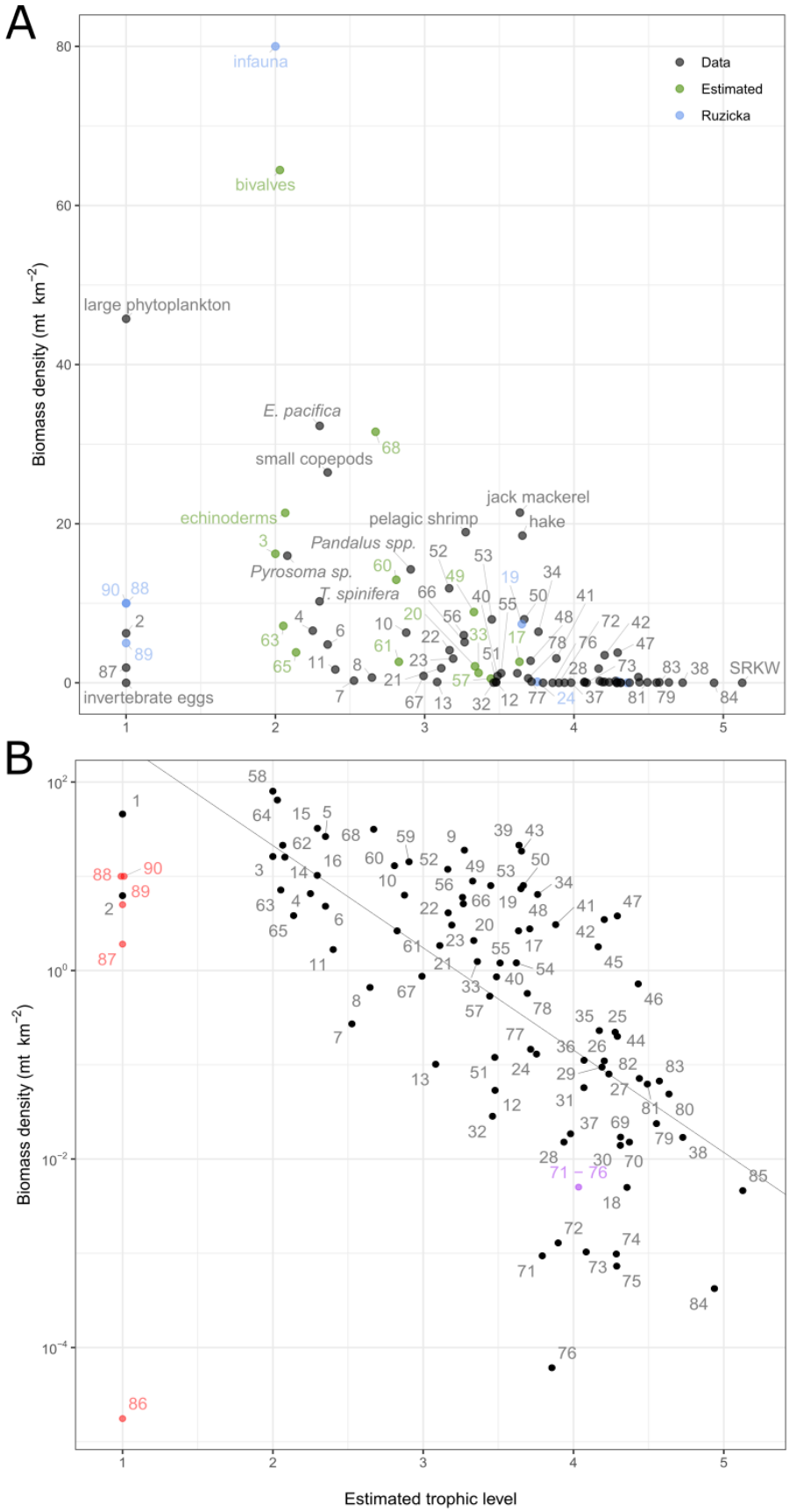
A
Data
Estimated
Ruzicka
infauna
bivalves
large phytoplankton
E. pacifica
small copepods
echinoderms
pelagic shrimp
jack mackerel
hake
Pandalus spp.
Pyrosoma sp.
T. spinifera
invertebrate eggs
SRKW
Biomass density (mt km^{-2})
B
Estimated trophic level

Fig 4: Biomass density and trophic level of model functional groups

A) Ecosystem-wide biomass density input values (y-axis) for the aggregated ecosystem model (no subregion-specific values) are based on survey data / stock assessments (black points), were borrowed from a previous ecosystem model (Ruzicka et al. 2012; blue points), or are estimated by the model during mass-balancing (green points; see methods). The trophic level of each functional group is estimated by the model and is based on the diet matrix. Numbers indicate functional groups, identified in Table 1. B) Same as A, but on a log (base 10) axis scale. Red points indicate detritus groups, which are not used in estimation of the regression line (Link 2010). Purple point is aggregated seabird groups 71 - 76 to display how the choice to aggregate groups affects how far away from the line the point falls. Equation for slope is estimated only with black points and is defined as $\log(y) = 3.5 - 1.085\ x$.

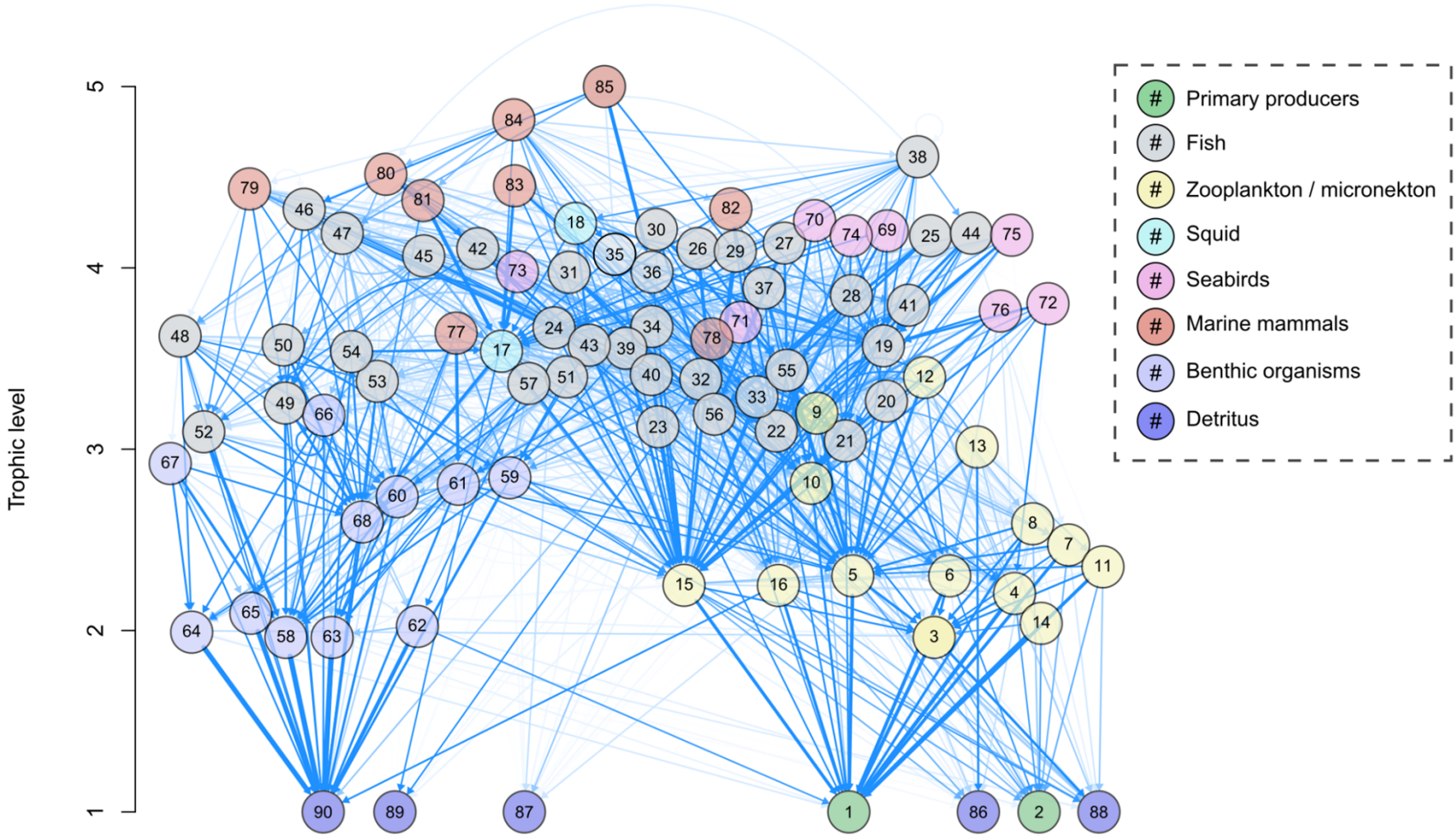
Trophic level
5
4
3
2
1
Primary producers
Fish
Zooplankton / micronekton
Squid
Seabirds
Marine mammals
Benthic organisms
Detritus

Fig 5: Diet matrix of ecosystem model by trophic level

The diet matrix is visualized here as a weighted, directed graph. Numbered nodes are functional groups (see Table 1 for functional group numbers), whereas arrows indicate directed edges from predator group towards prey group. The shade of blue indicates strength of interaction (higher diet preference results in darker blue network edges) up to a value of 0.10, at which point network edges get thicker with higher values. This aesthetic choice was made to not overly clutter the diagram and to make visualization of strong interactions more apparent. The y-axis values are the estimated trophic level of each functional group, and the x-axis is value-less and only used to help visualize multiple groups.

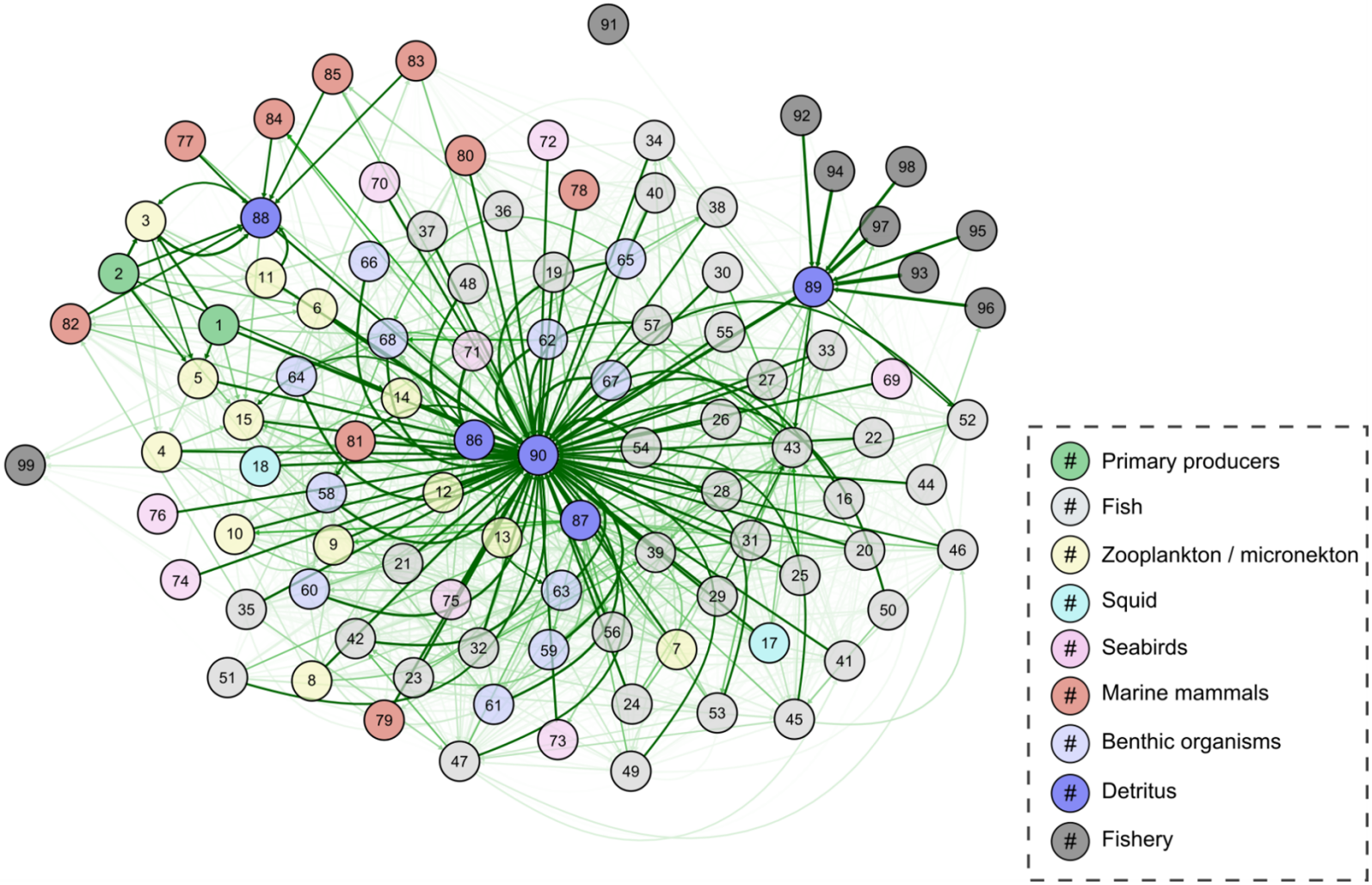
Primary producers
Fish
Zooplankton / micronekton
Squid
Seabirds
Marine mammals
Benthic organisms
Detritus
Fishery

Fig 6: EcoTran trophic network of ecosystem model

The EcoTran trophic network is visualized here as a weighted, directed graph. Numbered nodes are functional groups (see Table 1 for numbers), while arrows indicate directed edges (energy flows from producer groups towards consumer groups). The shade of green indicates strength of interaction (higher diet preference and prey biomass results in darker green network edges) up to a value of 0.10, at which point network edges get thicker with higher values, as in Fig 5. This graph includes detritus groups (86-90), which dominate the network.

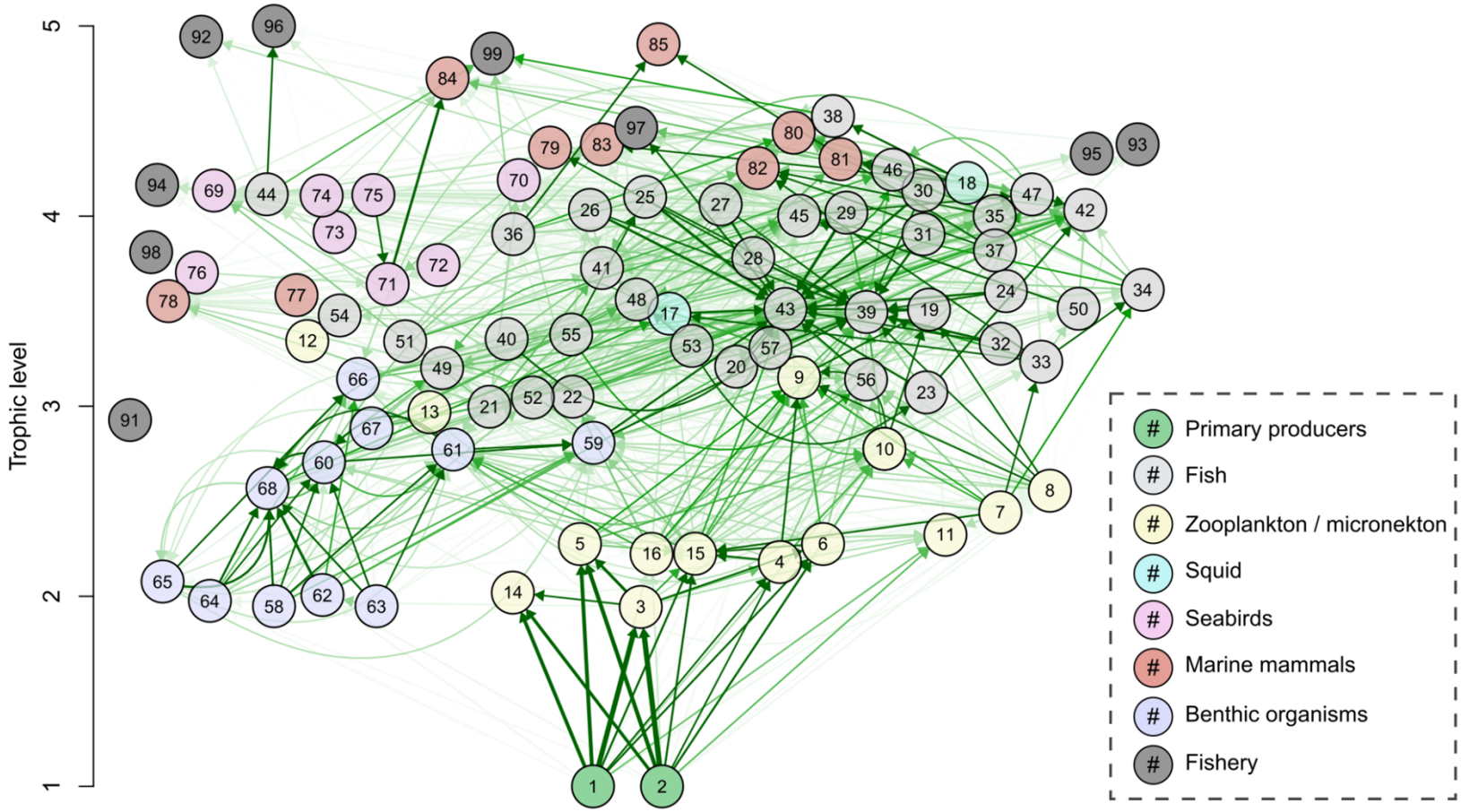

Fig 7: EcoTran trophic network of non-detritus groups by trophic level

The EcoTran trophic network is visualized here as a weighted, directed graph with detritus groups (86-90) removed (see Fig 6). Numbered nodes are functional groups (see Table 1 for numbers); arrows indicate directed edges (energy flows from producer groups

towards consumer groups). The shade of green indicates strength of interaction (higher diet preference and prey biomass results in darker green network edges) up to a value of 0.025, at which point network edges get thicker with higher values.

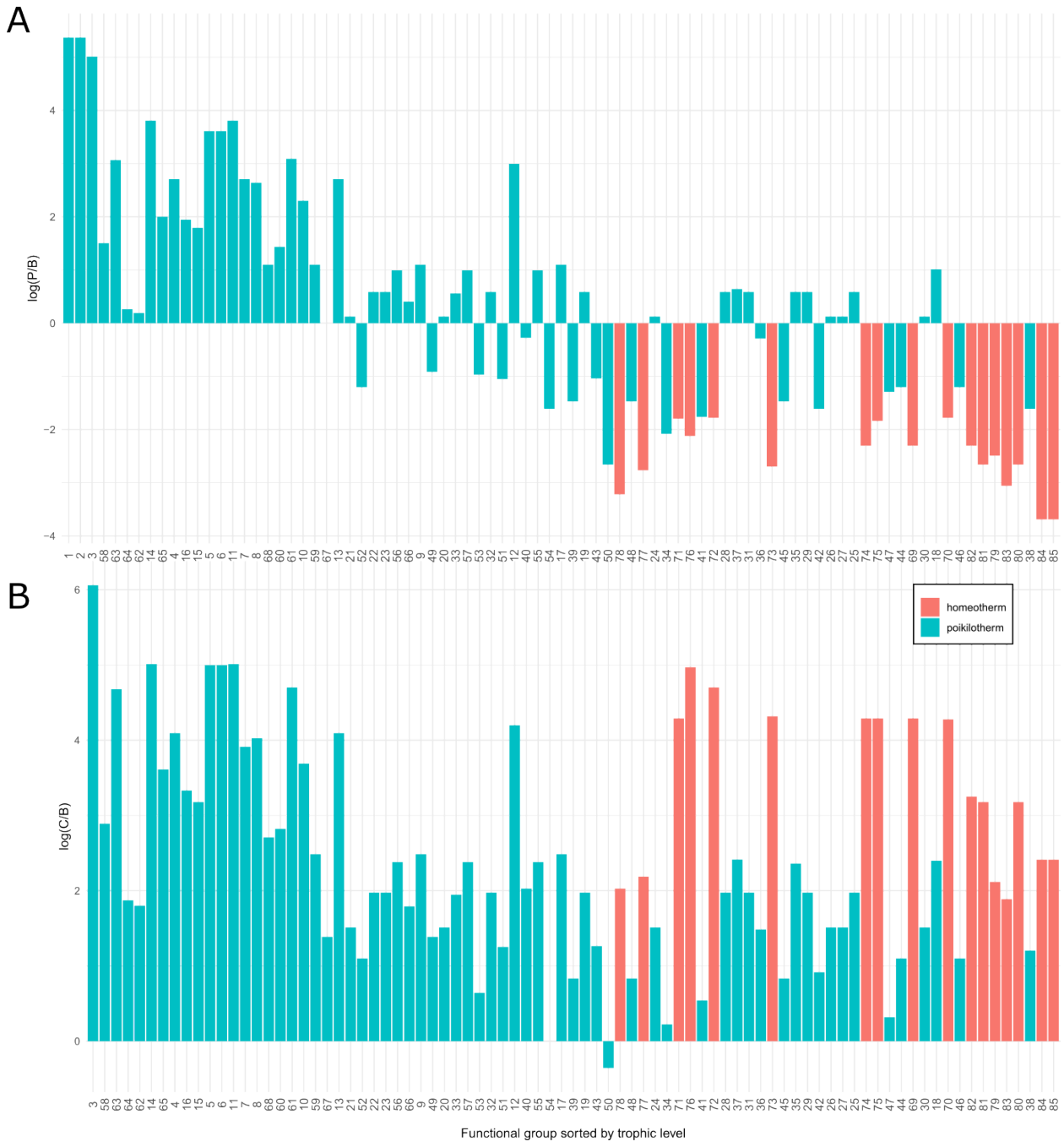

Fig 8: Validation; Biomass-specific production and consumption values by trophic level

(A) The y-axis is the log-scaled production to biomass ratio (biomass-specific production) and the x-axis numbers indicate the different functional groups (see Table 1) sorted by increasing trophic level (far left is low trophic levels, e.g., phytoplankton, and far right is high trophic levels, e.g., marine mammals). (B)

The y-axis is the log-scaled consumption to biomass ratio (biomass-specific consumption) and the x-axis is the same as in panel A. The y axes are on the log scale, so negative values indicate P/B and C/B values (for A and B, respectively) less than 1 on the original scale.

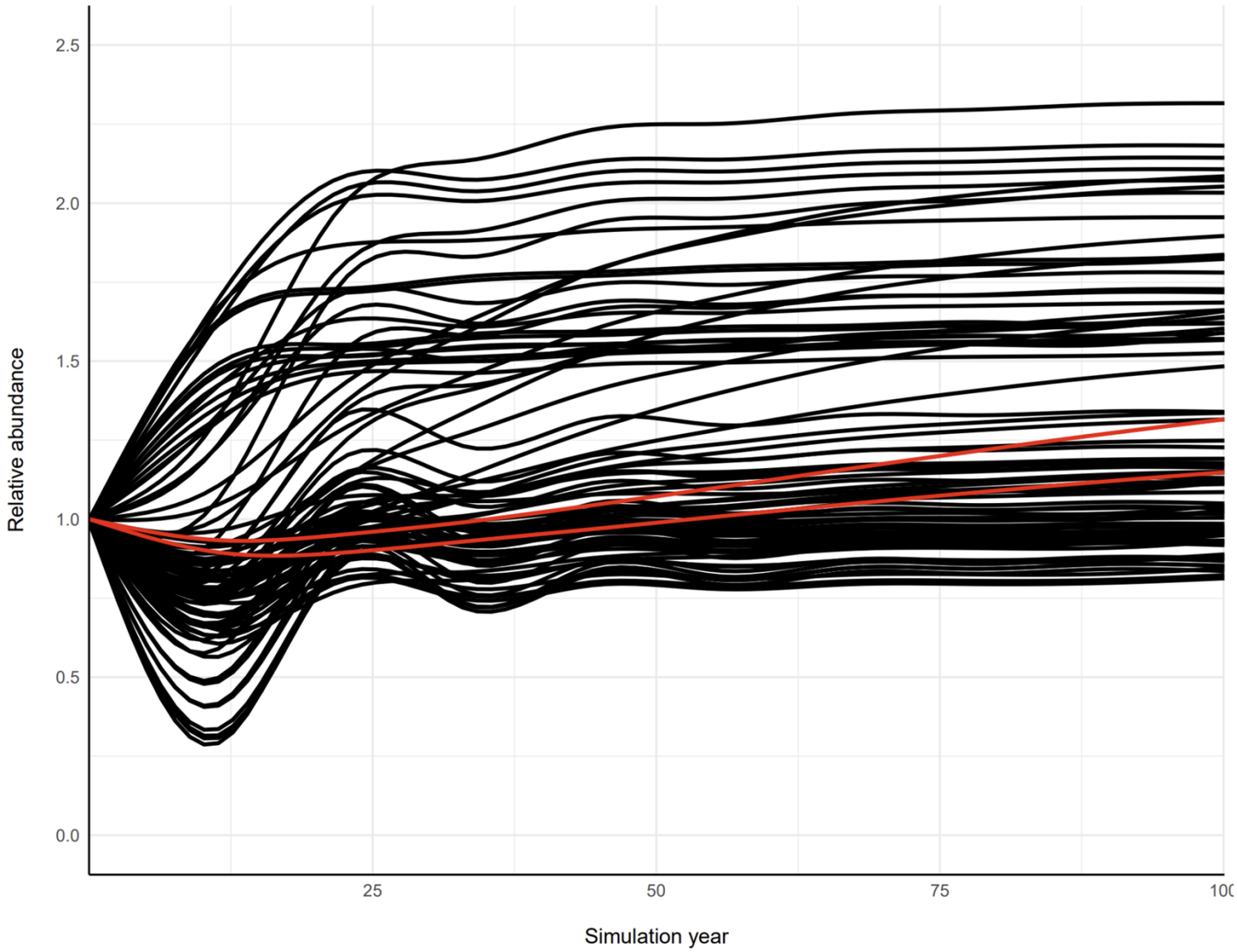
2.5
2.0
1.5
1.0
0.5
0.0
Relative abundance
25
50
75
100
Simulation year

Fig 9: 100-year model simulation driven by average upwelling time series

Each living consumer functional group is pictured here as a smoothed individual line. The proportion of abundance relative to starting values are plotted on the y-axis and the daily simulation timestep is plotted on the x-axis (axis in yearly units). The simulation here is driven by the average (day of year average for 1988-2021) Coastal Upwelling Transport Index (CUTI) to reduce interannual variation for assessment of equilibrium and model stability. Functional groups in red (both killer whale groups) indicate that populations are increasing by more than 5% in the final 20 years of simulation (other killer whales = 6.9%, Southern resident killer whales = 5.0%, followed by large toothed whales = 4.7% and sea lions = 4.4%; see Table S6 for all groups). All other groups have reached equilibrium (i.e., are within this 5% threshold). No functional groups go extinct over the 100-year simulation. See Fig S2 for similar simulation driven instead by a constant time series.

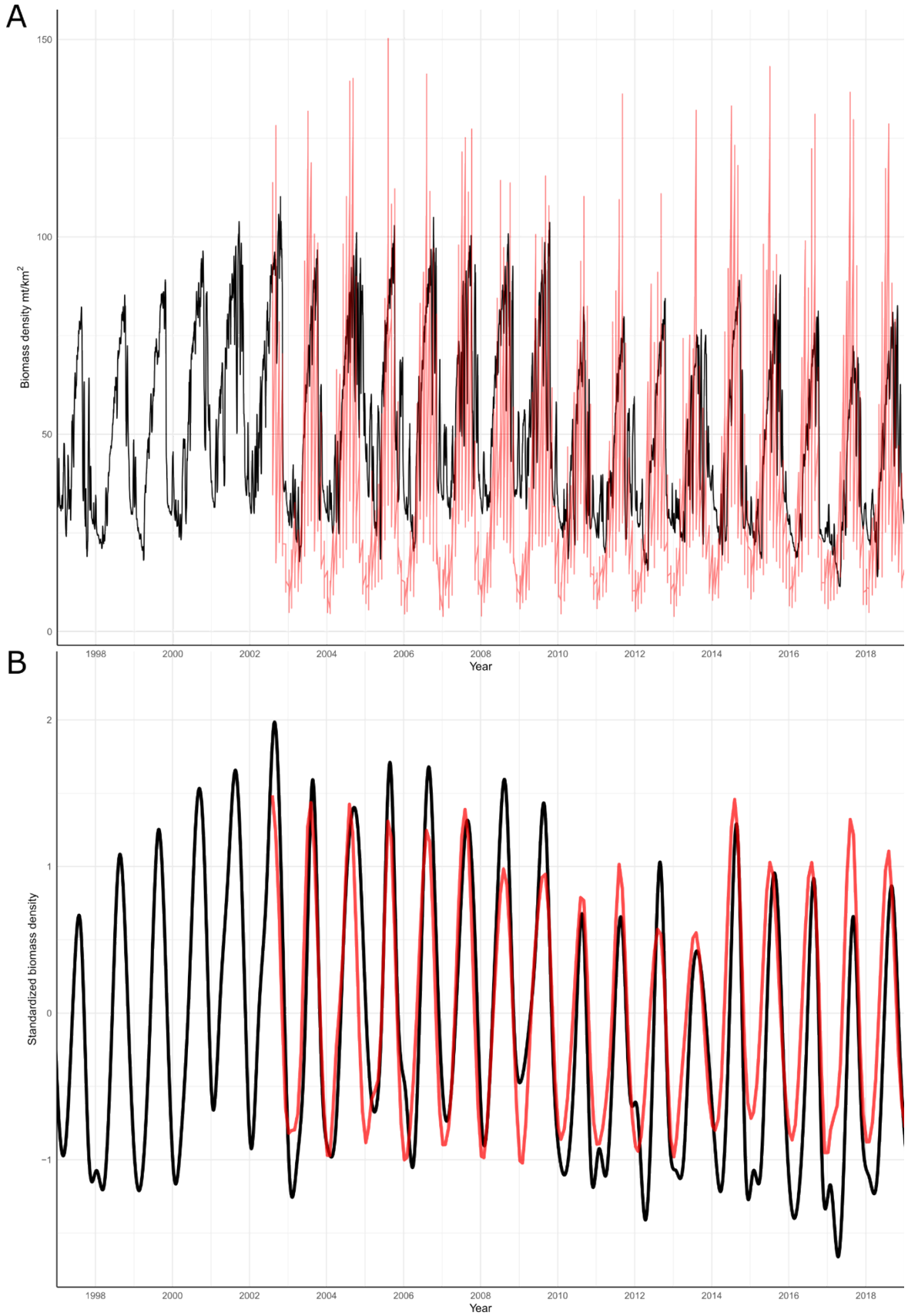
A
150
100
50
0
Biomass density mt/km^2
1998
2000
2002
2004
2006
2008
2010
2012
2014
2016
2018
Year
B
2
1
0
−1
Standardized biomass density
1998
2000
2002
2004
2006
2008
2010
2012
2014
2016
2018
Year

Fig 10: Primary production time series as both ecosystem model output and vertically generalized production model

Satellite imagery-derived estimates of primary productivity via a vertically generalized production model (VGPM, red lines) [49,50] are plotted against ecosystem model-derived estimates of primary production driven by an upwelling time series (black lines are aggregated large and small phytoplankton functional groups). The average values of the final eight years of the VGPM (2014 - 2021) are used to inform the starting conditions (values) for the ecosystem model. After this point, the ecosystem model is driven entirely by nutrient inputs to the system as determined by the coastal upwelling transport index (CUTI) [41], and any resemblance to the VGPM time series is an indication that the ecosystem model is capturing the appropriate dynamics in primary productivity. The primary production time series, in turn, is what drives the rest of the food web via bottom-up energy flow to higher trophic levels. Raw values are plotted in panel A, demonstrating the overlap in scale of values. Standardized (centered and scaled by 1 SD) values are shown in panel B to demonstrate the alignment of periodicity between our model and the VGPM.